Pre-carbonized nitrogen-rich polytriazines for the controlled growth of silver nanoparticles: catalysts for enhanced CO_2 chemical conversion at atmospheric pressure

Jian Liu[a,*], Xiaoyi Zhang[a], Bingyan Wen[a], Yipei Li[a], Jingjing Wu[a], Zhipeng Wang[a], Ting Wu[a], Rusong, Zhao[b,c], Shenghong Yang[b,*]

[a]*Institute of Advanced Materials, College of Chemistry and Chemical Engineering, Jiangxi Normal University, Nanchang, 330022, China.*

[b]*Shandong Provincial Key Laboratory of Molecular Engineering, School of Chemistry and Chemical Engineering, Qilu University of Technology (Shandong Academy of Sciences), Jinan 250014, China.*

[c]*Key Laboratory for Applied Technology of Sophisticated Analytical Instruments of Shandong Province, Analysis and Test Center, Qilu University of Technology (Shandong Academy of Sciences), Jinan 250014, China*

*Corresponding author.

E-mail: jianliu18@jxnu.edu.cn; zhaors1976@126.com; yangsh@qlu.edu.cn.

Section 1: Characterization data of polytriazines and Ag@polytriazines

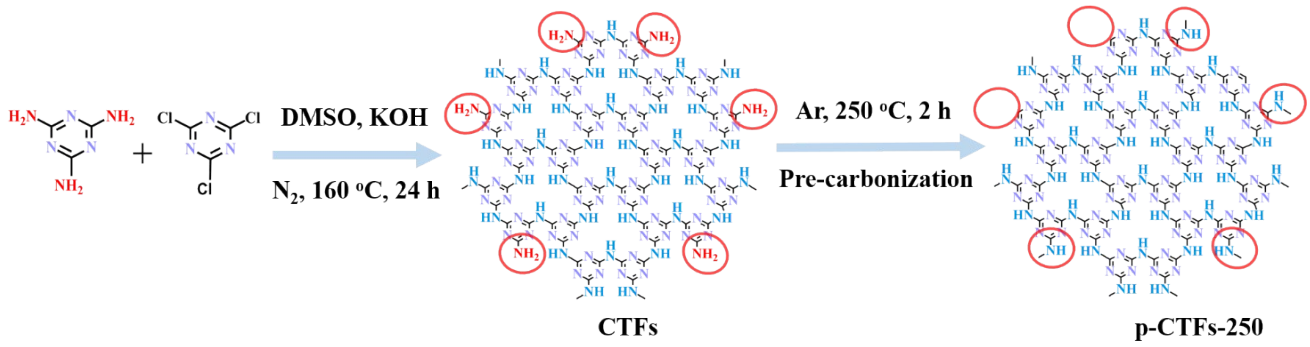

Scheme S1. Synthetic route of typical p-CTFs-250. primary amino groups (-NH_2) were decomposed or condensed.

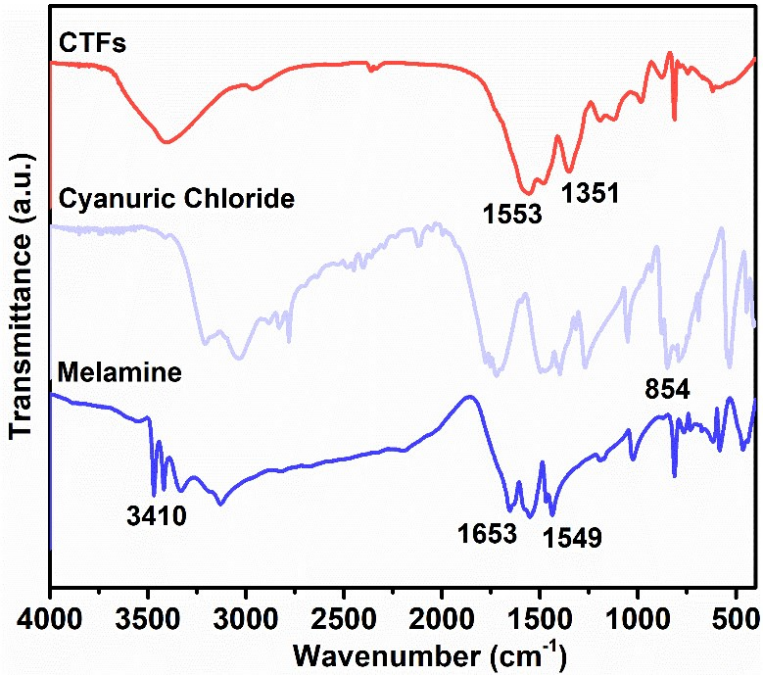

Figure S1. FT-IR spectra of melamine, cyanuric chloride, and CTFs.

The successful formation of CTFs was first confirmed using FT-IR spectroscopy in Figure S1. It showed a representative peak for C–NH–C stretching vibration (1351 cm^{-1}) in CTFs along with the absence of the band for C−Cl stretching vibration in cyanuric chloride (854 cm^{-1}), indicating that two triazine rings were coupled by –NH– through HCl molecule removal. The peak at 814 cm^{-1} is attributed to the deformation

vibrations of the triazine ring [1]. Only a broadband at 3410 cm^{-1} region in CTFs, instead of multiple bands for melamine, is related to the N–H (C–NH–C/ C–NH_2) in condensed copolymers [2]. Similarly, the broad band at 1553 cm^{-1} belongs to the coupling vibration between C=N and N–H, which is different from the C=N stretching vibration at 1549 cm^{-1} and the –NH_2 bending vibration at 1653 cm^{-1} in melamine [3].

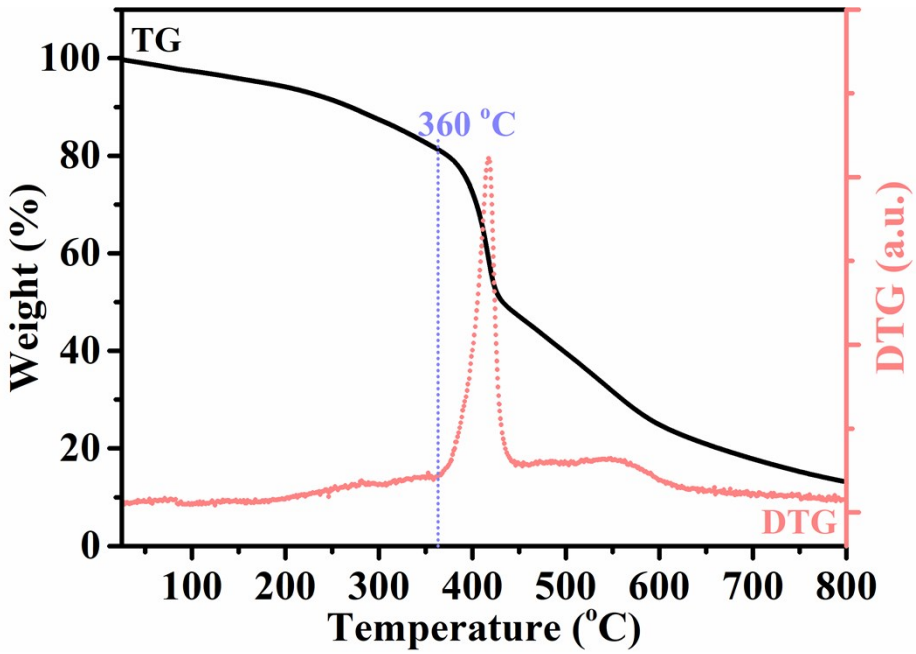

Figure S2. TG and DTG curves of CTFs.

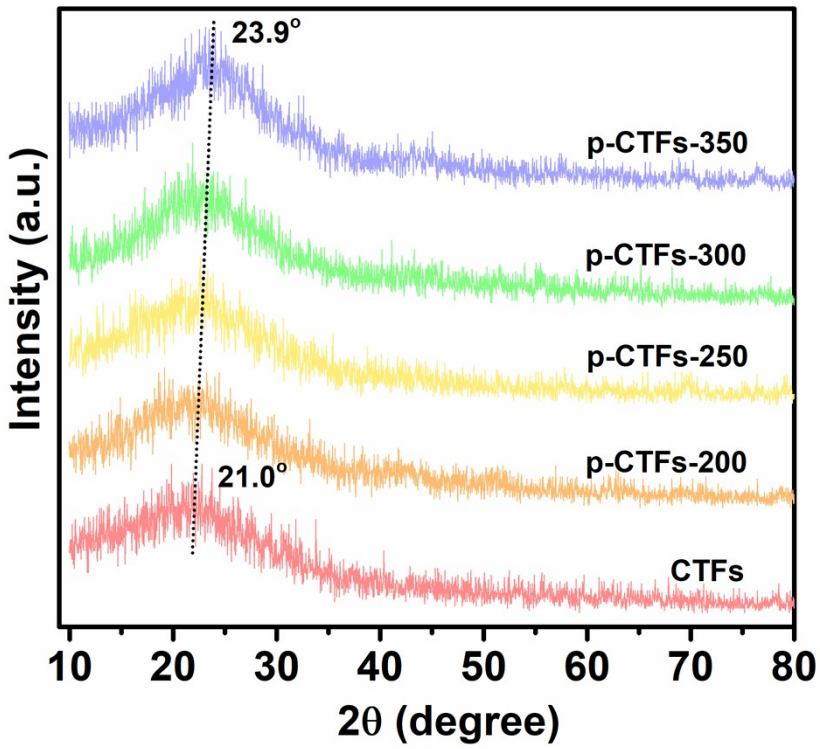

Figure S3. XRD spectra of CTFs and p-CTFs-x.

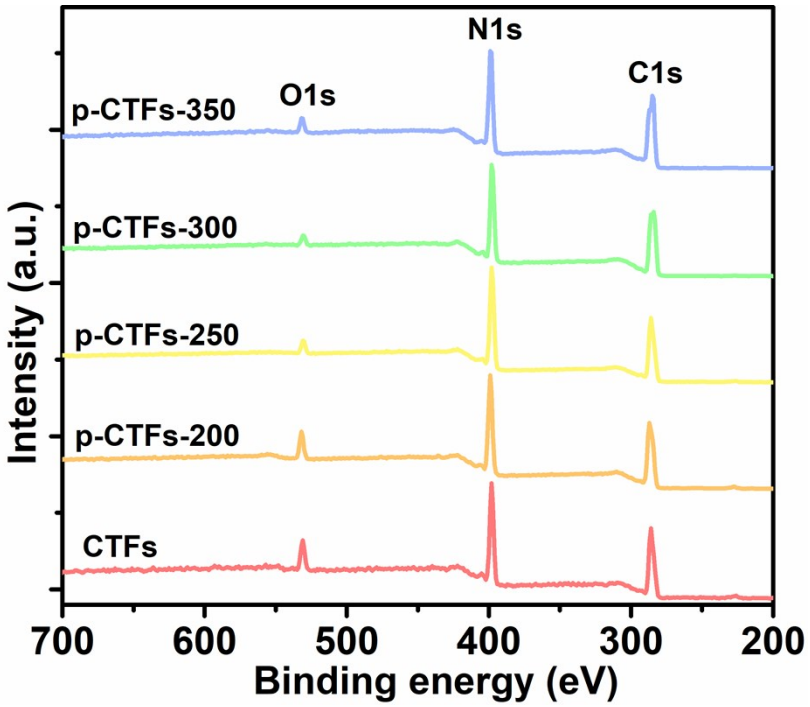

Figure S4. XPS spectra of CTFs and CTFs-T.

Table S1. Chemical compositions and nitrogen functional groups from XPS data of CTFs and p-CTFs-*x*.

Samples	Elemental analysis (wt%)				at.% of total N1s			
	C	*N*	*H*	*O and other elements*	*-C=N-*	*-C-NH- -C-NH$_2$*	*N-(C)3*	*π-π* satellite*
CTFs	34.73	58.98	4.74	1.55	35.5	60.2	0	4.3
p-CTFs-200	35.78	58.10	4.46	1.66	36.0	59.4	0	4.6
p-CTFs-250	37.52	56.95	4.43	1.10	36.6	58.3	0	5.1
p-CTFs-300	38.19	56.24	4.42	1.15	43.7	50.4	0	5.9
p-CTFs-350	39.61	55.65	3.77	0.97	42.4	39.4	10.6	7.6

Determination of the vanishing of –NH_2 groups in polytriazines

Diazotization reaction: mixture of polytriazine (0.75 ml, 0.5 mg ml^{-1}), $NaNO_2$ (0.75 ml, 1 mg ml^{-1}), and H_2SO_4 (0.75 ml, 0.1 M) was stirred 1 h at 0 °C. Then $Na_2B_4O_7$-NaOH buffer solution (3 ml, 0.08 M-0.12M)) and α-naphthol (0.75 ml, 1 mg ml^{-1}) were added quickly and incubated 30 min at 50 °C. The suspensions were used directly for fluorescence detection. (E_x = 340 nm, E_m = 466 nm) Controlled experiments were conducted by replacing $NaNO_2$ with equal volume of H_2O.

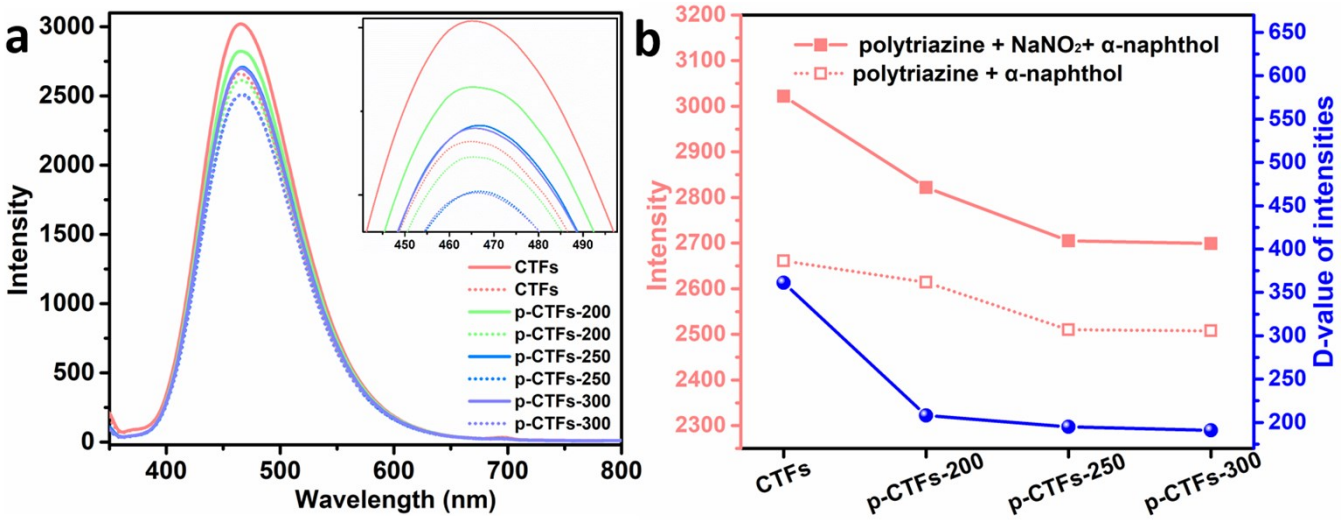

Figure S5. (a) the fluorescence spectra of α-naphthol in different polytriazine conditions with $NaNO_2$ (solid lines) or without $NaNO_2$ (dashed lines). (b) the corresponding intensity values (E_m = 466 nm) and the D-value of the intensities.

Diazotization reaction between the –NH_2 groups in polytriazines and NO_2^- in acidic medium will generate aryl diazonium salt, which will further couple with α-naphthol in basic medium (pH ≈ 8.0) and enhance the fluorescence intensity of α-naphthol due to the electrophilicity of the aryl diazonium salt [4]. As shown in Figure S5, the fluorescence intensity of α-naphthol increased obviously in alkaline aqueous condition after CTFs treated with NO_2^- in acidic medium. The D-values of intensities were not further changed when polytriazines (p-CTFs-250 and p-CTFs-300) were introduced, indicating that no –NH_2 groups were remained there.

Table S2. BET surface area and CO_2 sorption capacity of polytriazines and other porous materials.

Materials	BET surfaces area (m^2 g^{-1})	CO_2 up take at at 298 K and 1 atm. (mg g^{-1})	CO_2 sorption capacity in per unit BET surface area (mg m^{-2})	*Ref.*
CTFs	667.7	61.9	0.093	*This work*
p-CTFs-200	615.7	65.0	0.106	
p-CTFs-250	532.5	74.1	0.139	
p-CTFs-300	416.7	40.2	0.096	
p-CTFs-350	83.2	23.3	0.280	
Ag@CTFs	575.6	55.6	0.097	
Ag@p-CTFs-250	455.0	63.5	0.140	
Ag@ p-CTFs-350	13.3	13.9	1.045	
3AM3CL	894	88	0.098	***5***
PAN-N2	1035	98.2	0.095	***6***
MIL-101	3083	96.8	0.031	***7***
POP-Byp	1123	70	0.062	***8***
NENP-1-350	880	182	0.206	***9***
CTF-DEC	1355	165	0.121	***10***
IISERP-COF	1230	96.5	0.078	***11***
Ag/PCNF-600	96	32.406	0.338	***12***
KAPS-Py	199	47.725	0.239	***13***
MIL-100(Fe)	1828	63.83	0.035	***14***
ZIF-8	1670	37.4	0.022	***15***

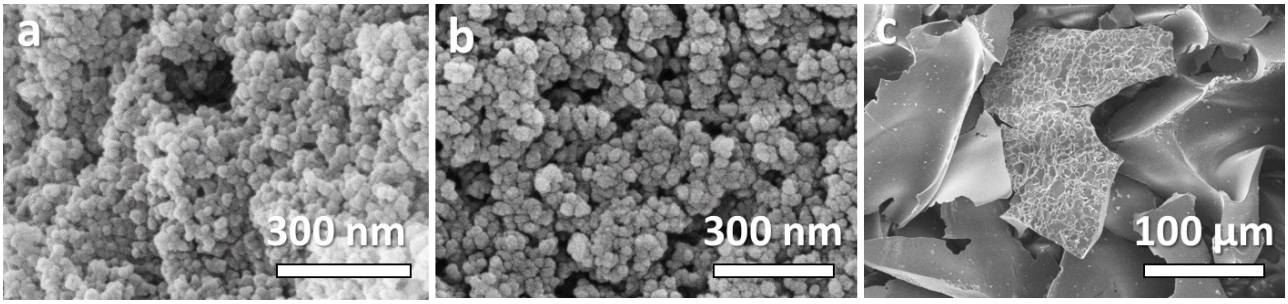

Figure S6. SEM images of (a) Ag@CTFs, (b) Ag@p-CTFs-250, (c) Ag@p-CTFs-350.

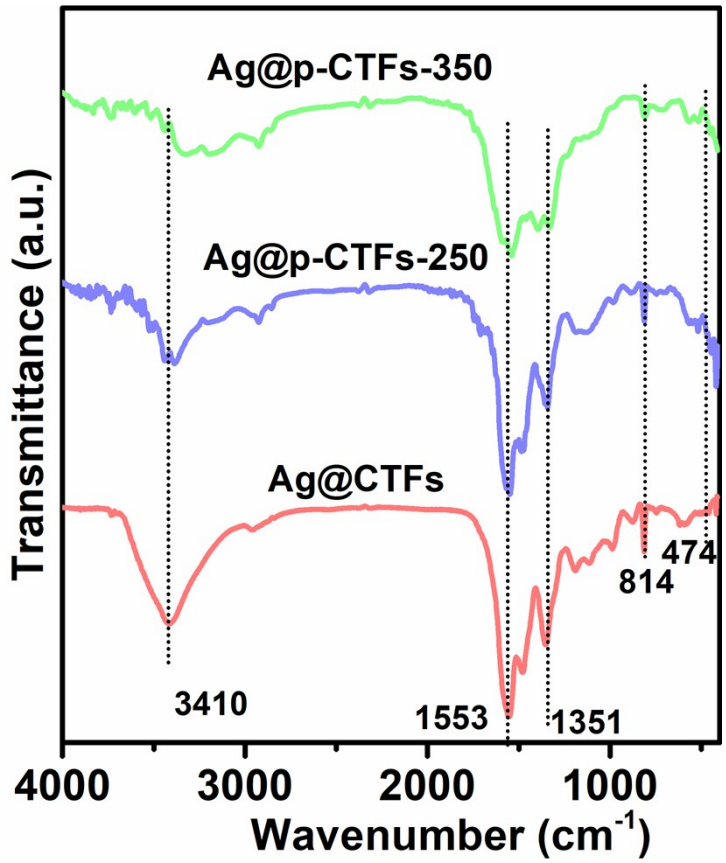

Figure S7. FT-IR spectra of Ag@CTFs, Ag@p-CTFs-250, and Ag@p-CTFs-350.

Section 2: Catalysis performance for the carboxylation of terminal alkynes

Table S3. Comparison with previous reported catalysts for 3-phenylpropiolic acid from CO_2 and 1-ethynylbenzene.

Entry	Catalyst	CO_2 pressure (atm)	Runs	Yield(%)[b]	*Ref.*
1	AgI	15	-	92	***16***
2	Ag@P-NHC	1	5	98	***17***
3	Ag(I)	1	-	91	***18***
4	-	2.5	-	95	***19***
5	Ag@MIL-101	1	5	96.5	***7***
6	rare-earth metal complexes	1	-	94	***20***
7	Ag_2WO_4	1	-	96	***21***
8	AgNPs@C_O-MOF	1	6	96	***22***
9	Ag_2O/NHC	1	-	98	***23***

10	Ag@MIL-100(Fe)	1	5	94.6	***14***
11	Ag@UIO-66(Zr)	1	5	98.7	***14***
12	Ag/Schiff-SiO_2	1	-	98	***24***
13	Ag/KAPs-P	1	5	92	***13***
14	CTF-DCE-Ag	1	-	90.2	***10***
15	Ag^0@CTFN	1	6	97	***25***
16	Ag@NOMP	1	5	96	***26***
17	Ag/PCNF-T	1	5	90	***12***
18	UiO-66@UiO-67-BPY-Ag	1	5	96	***27***
19	TBAA- CH_3CN(no metal)	10	-	85	***28***
20	Ag@PHNCT	1	5	98	***29***
21	Ag@p-CTFs-250	1	5	96	***This work***

Reference

[1] T. Komatsu, Attempted chemical synthesis of graphite-like carbon nitride, J. Mater. Chem. 11 (2001) 799-801.

[2] S.M. Lyth, Y. Nabae, S. Moriya, S. Kuroki, M.A. Kakimoto, J.I. Ozaki, S. Miyata, Carbon nitride as a nonprecious catalyst for electrochemical oxygen reduction. J. Phys. Chem. C 113 (2009) 20148-20151.

[3] Y. Cui, J. Zhang, G. Zhang, J. Huang, P. Liu, M. Antonietti, X. Wang, Synthesis of bulk and nanoporous carbon nitride polymers from ammonium thiocyanate for photocatalytic hydrogen evolution, J. Mater. Chem. 21 (2011) 13032–13039.

[4] K.J. Johnston, A.E. Ashford, A simultaneous-coupling azo dye method for the quantitative assay of esterase using α-naphthyl acetate as substrate, Histochem. J. 12 (1980), 221-234.

[5] S.C. Qi, J.K. Wu, J. Lu, G.X. Yu, R.R. Zhu, Y. Liu, X.Q. Liu, L.B. Sun, Underlying mechanism of CO_2 adsorption onto conjugated azacyclo-copolymers: N-doped adsorbents capture CO_2 chiefly through acid–base interaction? J. Mater. Chem. A 7 (2019) 17842-17853.

[6] G. Li, X. Zhou, Z. Wang, Highly nitrogen-rich microporous polyaminals using N, N-dimethylformamide and formamide as the starting monomers for CO_2 adsorption and separation, J. Phys. Chem. C 124 (2020) 3087-3094.

[7] X.H. Liu, J.G. Ma, Z. Niu, G. M. Yang, P. Cheng, An efficient nanoscale heterogeneous catalyst for the capture and conversion of carbon dioxide at ambient pressure, Angew. Chem. Int. Ed. 54 (2015) 988-991.

[8] Z. Dai, Q. Sun, X. Liu, L. Guo, J. Li, S. Pan, C. Bian, L. Wang, Xin. Hu, X. Meng, L .Zhao, F. Deng, F.S. Xiao, A hierarchical bipyridine-constructed framework for highly efficient carbon dioxide capture and catalytic conversion, ChemSusChem 10 (2017) 1186-1192.

[9] M. Chaudhary, P. Mohanty, Pre-carbonization: an efficient route to improve the textural and gas sorption properties of nitrogen-enriched nanoporous polytriazine, ChemNanoMa 6 (2020) 113-117.

[10] Q.Q. Dang, C.Y. Liu, X.M. Wang, X.M. Zhang, Novel covalent triazine framework for high-performance CO_2 capture and alkyne carboxylation reaction, ACS Appl. Mater. Interfaces 10 (2018) 27972-27978.

[11] D. Chakraborty, P. Shekhar, H.D. Singh, R. Kushwaha, C.P. Vinod, R. Vaidhyanathan, Ag nanoparticles supported on a resorcinol-phenylenediamine-based covalent organic framework for chemical fixation of CO_2, Chem. Asian J. 14 (2019) 4767-4773.

[12] X. Lan, Y. Li, C. Du, T. She, Q. Li, G. Bai, Porous carbon nitride frameworks derived from covalent triazine framework anchored Ag nanoparticles for catalytic CO_2 conversion, Chem. Eur. J. 25 (2019) 8560-8569.

[13] Z. Wu, Q. Liu, X. Yang, X. Ye, H. Duan, J. Zhang, Bo. Zhao, Y. Huang, Knitting aryl network polymers-incorporated Ag nanoparticles: a mild and efficient catalyst for the fixation of CO_2 as carboxylic acid, ACS Sustainable Chem. Eng. 5(2017) 9634-9639.

[14] N.N. Zhu, X.H. Liu, T. Li, J.G. Ma, P. Cheng, G.M. Yang, Composite system of Ag nanoparticles and metal–organic frameworks for the capture and conversion of carbon dioxide under mild conditions, Inorg. Chem. 56 (2017) 3414-3420.

[15] J. Shi, L. Zhang, N. Sun, D. Hu, Q. Shen, F. Mao, Q. Gao, W. Wei, Facile and rapid preparation of Ag@ZIF-8 for carboxylation of terminal alkynes with CO_2 in mild conditions, ACS Appl. Mater. Interfaces 11 (2019) 28858-28867.

[16] X. Zhang, W.Z. Zhang, X. Ren, L.L. Zhang, X.B. Lu, Ligand-free Ag(I)-catalyzed carboxylation of terminal alkynes with CO_2, Org.Lett. 13 (2011) 2402-2405.

[17] D. Yu, M.X. Tan, Y. Zhang, Carboxylation of terminal alkynes with carbon dioxide catalyzed by poly(N-heterocyclic carbene)-supported silver nanoparticles, Adv. Synth. Catal. 354(2012) 969-974.

[18] M. Arndt, E. Risto, T. Krause, L. Gooßen, C-H carboxylation of terminal alkynes catalyzed by low loadings of silver(I)/DMSO at ambient CO_2 pressure, ChemCatChem. 4 (2012) 484-487.

[19] D. Y. Yu, Y.G. Zhang, The direct carboxylation of terminal alkynes with carbon dioxide, Green Chem. 13 (2011) 1275-1279.

[20] M.X. Tan, L.Q. Gu, N.N. Li, J.Y. Ying, Y.G. Zhang, Mesoporous poly-melamine-formaldehyde (mPMF) – a highly efficient catalyst for chemoselective acetalization of aldehydes, Green Chem. 15 (2013) 1127-1132.

[21] L.H. Yang, H.M. Wang, Recent advances in carbon dioxide capture, fixation, and activation by using N-heterocyclic carbenes, ChemSusChem. 7 (2014) 962-998.

[22] X.H. Liu, J.G. Ma, Z. Niu, G.M. Yang, P. Cheng, An efficient nanoscale heterogeneous catalyst for the capture and conversion of carbon dioxide at ambient pressure, Angew. Chem. Int. Ed. 53 (2014) 1-5.

[23] H. Cheng, B. Zhao, Y. Yao, C. Lu, Carboxylation of terminal alkynes with carbon dioxide catalyzed by bridged bis(amidate) rare-earth metal amides, Green Chem. (2014).

[24] C.X. Guo, B. Yu, J.N. Xie, L.N. He, Silver tungstate: a single-component bifunctional catalyst for carboxylation of terminal alkynes with CO_2 in ambient conditions, Green Chem. 17 (2015) 474-479.

[25] M. Cui, Q. Qian, Z. He, J. Ma, X. Kang, J. Hu, Z. Liu, B. Han, Synthesizing Ag nanoparticles of small size on a hierarchical porosity support for the carboxylative cyclization of propargyl alcohols with CO_2 under ambient conditions, Chem. Eur. J. 21 (2015) 15924-15928.

[26] Y. Zhang, D.S. Lim, Synergistic carbon dioxide capture and conversion in porous materials, ChemSus Chem. 8 (2015) 2606-2608.

[27] R.A. Molla, K. Ghosh, B. Banerjee, M.A. Iqubal, S.K. Kundu, S.M. Islam, A. Bhaumik, Silver nanoparticles embedded over porous metal organic frameworks for carbon dioxide fixation via carboxylation of terminal alkynes at ambient pressure, J. Colloid Interface Sci. 477 (2016) 220-229.

[28] Y. Yuan, C. Chen, C. Zeng, B. Mousavi, S. Chaemchuen, F. Verpoort, Carboxylation of terminal alkynes

with carbon dioxide catalyzed by an in situ Ag_2O/N-heterocyclic carbene precursor system, ChemCatChem 9 (2017) 882-887.
[29] N.N. Zhu, X.H. Liu, T. Li, J.G. Ma, P. Cheng, G.M. Yang, Composite system of Ag nanoparticles and metal–organic frameworks for the capture and conversion of carbon dioxide under mild conditions, Inorg. Chem. 56 (2017) 3414-3420.
[30] Z. Wu, L. Sun, Q. Liu, X. Yang, X. Ye, Y. Hu, Y. Huang, A schiff base-modified silver catalyst for efficient fixation of CO_2 as carboxylic acid at ambient pressure, Green Chem. 19 (2017) 2080-2085.
[31] Z. Wu, Q. Liu, X. Yang, X. Ye, H. Duan, J. Zhang, B. Zhao, Y. Huang, Knitting aryl network polymers-incorporated Ag nanoparticles: a mild and efficient catalyst for the fixation of CO_2 as carboxylic acid, ACS Sustainable Chem. Eng. 5 (2017) 9634-9639.
[32] Q.Q. Dang, C.Y. Liu, X.M. Wang, X.M. Zhang, Novel covalent triazine framework for high-performance CO_2 capture and alkyne carboxylation reaction, ACS Appl. Mater. Interfaces. 10 (2018) 27972-27978.
[33] X. Lan, C. Du, L. Cao, T. She, Y. Li, G. Bai, Ultrafine Ag nanoparticles encapsulated by covalent triazine framework nanosheets for CO_2 conversion, ACS Appl. Mater. Interfaces. 10 (2018) 38953-38962.
[34] W. Zhang, Y. Mei, X. Huang, P. Wu, H. Wu, M. He, Size-controlled growth of silver nanoparticles onto functionalized ordered mesoporous polymers for efficient CO_2 upgrading, ACS Appl. Mater. Interfaces 11 (2019) 44241-44248.
[35] X. Lan, Y. Li, C. Du, T. She, Q. Li, G. Bai, Porous carbon nitride frameworks derived from covalent triazine framework anchored Ag nanoparticles for catalytic CO_2 conversion, Chem. Eur. J. 25 (2019) 8560-8569.
[36] Y. Gong, Y. Yuan, C. Chen, P. Zhang, J. Wang, S. Zhuiykov, S. Chaemchuen, F. Verpoort, Core-shell metal-organic frameworks and metal functionalization to access highest efficiency in catalytic carboxylation, J. Catal. 371 (2019) 106-115.
[37] D.J. Shah, A.S. Sharma, A.P. Shah, V.S. Sharma, M. Athar, J.Y. Soni, Fixation of CO_2 as a carboxylic acid precursor by microcrystalline cellulose (MCC) supported Ag NPs: a more efficient, sustainable, biodegradable and eco-friendly catalyst, New J. Chem. 43 (2019) 8669-8676.
[38] W.H. Wang, X. Feng, K. Sui, D. Fang, M. Bao, Transition metal-free carboxylation of terminal alkynes with carbon dioxide through dual activation: synthesis of propiolic acids, J. CO_2 UTIL. 32 (2019) 140-145.
[39] X. Lan, Q. Li, L. Cao, C. Du, L. Ricardez-Sandoval, G. Bai, Rebuilding supramolecular aggregates to porous hollow N-doped carbon tube inlaid with ultrasmall Ag nanoparticles: a highly efficient catalyst for CO_2 conversion, Appl. Surf. Sci. 508 (2020) 145220.

Section 3: Characterization data of products

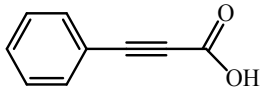

Compound **1**: White solid; ^{1}H NMR (400 MHz, $CDCl_3$) δ (ppm): 10.11 (br, s, 1H, ─COOH), 7.60–7.62 (m, 2H, Ar-H), 7.46–7.50 (m, 1H, Ar-H), 7.37–7.41 (m, 2H, Ar-H); ^{13}C NMR (100 MHz, $CDCl_3$) δ(ppm): 157.98 (─COOH), 132.97, 130.88, 128.39, 118.74, 88.55, 79.85.

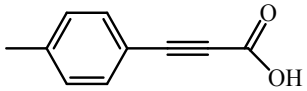

Compound **2**: White solid; ^{1}H NMR (400 MHz, $CDCl_3$) δ (ppm): 10.07 (br, s, 1H, ─COOH), 7.47–7.56 (m, 2H, Ar-H), 7.16–7.25 (m, 2H, Ar-H), 2.39 (s, 3H); ^{13}C NMR (100 MHz, $CDCl_3$) δ (ppm): 154.09 (─COOH), 132.97, 130.61, 128.54, 119.55, 86.05, 80.62, 14.07.

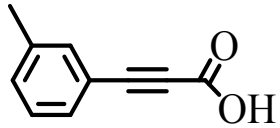

Compound **3**: White solid; ^{1}H NMR (400 MHz, $CDCl_3$) δ (ppm): 8.61 (br, s, 1H, ─COOH), 7.34–7.36 (m, 2H, Ar-H), 7.20–7.21 (m, 2H, Ar-H), 2.28 (s, 3H); ^{13}C NMR (100 MHz, $CDCl_3$) δ (ppm): 138.38 (─COOH), 133.66, 131.94, 130.31, 128.42, 118.77, 89.09, 79.82, 21.05.

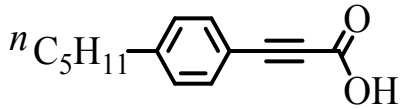

Compound **4**: White solid; ^{1}H NMR (400 MHz, $CDCl_3$) δ (ppm): 7.51–7.53 (m, 2H, Ar-H), 7.18–7.20 (m, 2H, Ar-H), 2.61 (t, J = 7.6 Hz, 2H), 1.28–1.60 (m, 6H), 0.87 (t, J = 7.6 Hz, 3H); ^{13}C NMR (100 MHz, $CDCl_3$) δ (ppm): 158.19 (─COOH), 146.95, 133.41, 128.70, 115.88, 89.72, 79.64, 36.17, 31.42, 30.71, 22.36, 13.95.

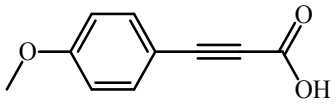

Compound **5**: White solid; ^{1}H NMR (400 MHz, *d*-DMSO) δ (ppm): 7.57–7.61 (m, 2H, Ar-H), 7.01–7.04 (m, 2H, Ar-H), 3.82 (s, 3H), 3.40 (br, s, 1H, ─COOH); ^{13}C NMR (100 MHz, *d*-DMSO) δ (ppm): 161.58 (─COOH), 154.94, 135.01, 115.19, 113.70, 85.63, 81.52, 55.53.

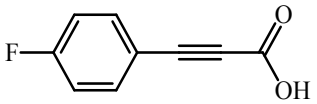

Compound **6**: White solid; ^{1}H NMR (400 MHz, *d*-DMSO) δ (ppm): 7.61–7.65 (m, 2H, Ar-H), 7.08–7.13 (m, 2H, Ar-H), 6.58 (br, s, 1H, ─COOH); ^{13}C NMR (100 MHz, *d*-DMSO) δ (ppm): 162.54 (─COOH), 154.80, 135.92, 117.09, 115.93, 83.93, 82.08.

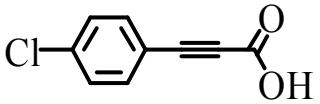

Compound **7**: White solid; ^{1}H NMR (400 MHz, *d*-DMSO) δ (ppm): 7.67-7.61 (m, 1H, Ar-H), 7.62–7.58 (m, 2H, Ar-H), 7.58-7.47 (m, 1H, Ar-H); ^{13}C NMR (100 MHz, *d*-DMSO) δ (ppm): 154.17 (─COOH), 133.53,

131.52, 130.23, 120.77, 87.19, 85.61.

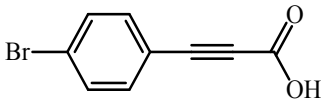

Compound **8**: White solid; ^{1}H NMR (400 MHz, *d*-DMSO) δ (ppm): 7.52-7.57 (m, 2H, Ar-H), 7.46-7.50 (m, 2H, Ar- H), 3.39 (br, s, 1H, ─COOH); ^{13}C NMR (100 MHz, *d*-DMSO): δ (ppm): 154.73 (─COOH), 134.96, 132.67, 125.20, 118.74, 83.55, 83.25.

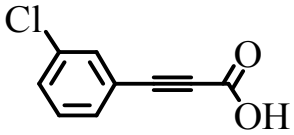

Compound **9**: White solid; ^{1}H NMR (400 MHz, *d*-DMSO) δ (ppm): 7.72-7.63 (m, 1H, Ar-H), 7.62-7.61 (m, 2H, Ar- H), 7.60-7.49 (m, 1H, Ar-H), 3.31 (br, s, 1H, ─COOH); ^{13}C NMR (100 MHz, *d*-DMSO): δ (ppm): 154.43 (─COOH), 153.91, 136.27, 134.09, 132.26, 121.45, 118.34, 83.51, 82.74.

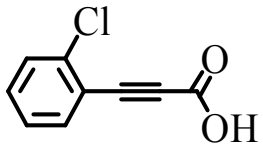

Compound **10**: White solid; ^{1}H NMR (400 MHz, *d*-DMSO) δ (ppm): 7.78-7.66 (m, 1H, Ar-H), 7.64 (m, 1H, Ar- H), 7.60-7.59 (m, 1H, Ar-H), 7.57-7.47 (m, 1H, Ar- H); ^{13}C NMR (100 MHz, *d*-DMSO): 154.55 (─COOH), 136.23, 135.17, 132.89, 130.15, 128.14, 119.54, 86.53, 80.97.

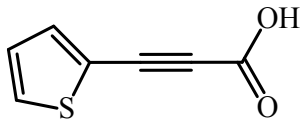

Compound **11**: Yellow solid; ^{1}H NMR (400 MHz, $CDCl_3$) δ (ppm): 8.86 (br, s, 1H, ─COOH), 7.52-7.56 (m, 2H, Ar-H), 7.07–7.10 (m, 1H, Ar-H); ^{13}C NMR (100 MHz, $CDCl_3$) δ (ppm): 158.10 (─COOH), 137.37, 133.82, 132.02, 127.67, 84.48, 82.93.

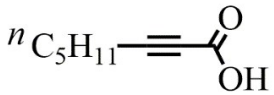

Compound **12**: ^{1}H NMR (400 MHz, $CDCl_3$) δ (ppm): 8.92 (br, s, 1H, -COOH), 2.35 (t, 6.8 Hz, 2H, CH_2), 1.63-1.59 (m, 2H, CH_2), 1.44-1.31 (m, 4H, CH_2), 0.93 (m, 6.4 , 3H, CH_3) ; ^{13}C NMR (100 MHz, $CDCl_3$) δ (ppm): 157.12 (-COOH), 91.36, 73.27, 32.1, 31.13, 22.27, 18.88, 14.04.

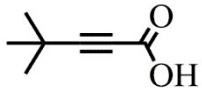

Compound **13**: ^{1}H NMR (400 MHz, $CDCl_3$) δ (ppm): 7.64 (br, s, 1H, -COOH), 1.31 (s, 9H, CH_3); ^{13}C NMR (100 MHz, $CDCl_3$) δ (ppm): 157.57 (-COOH), 98.78, 71.73, 30.08, 27.82.

Section 4: NMR spectral copies of products

Compound **1**

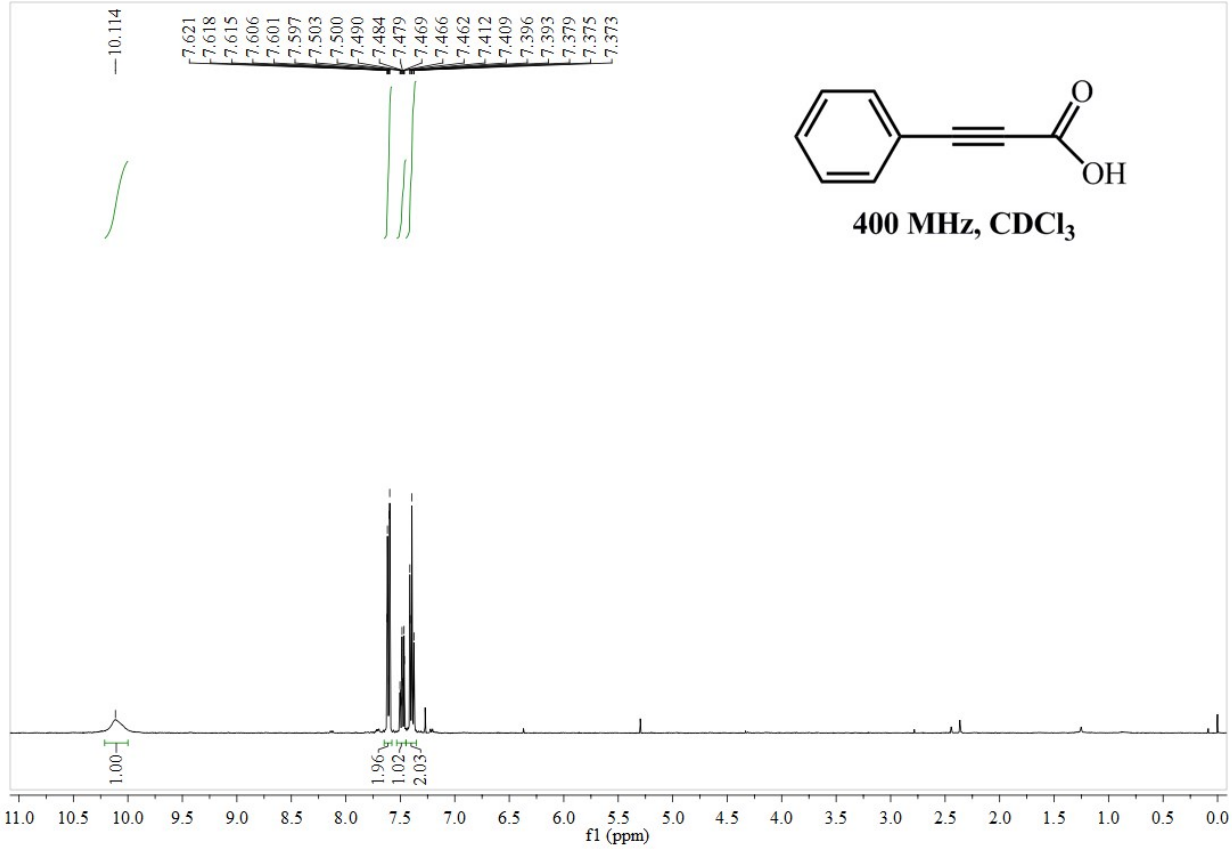

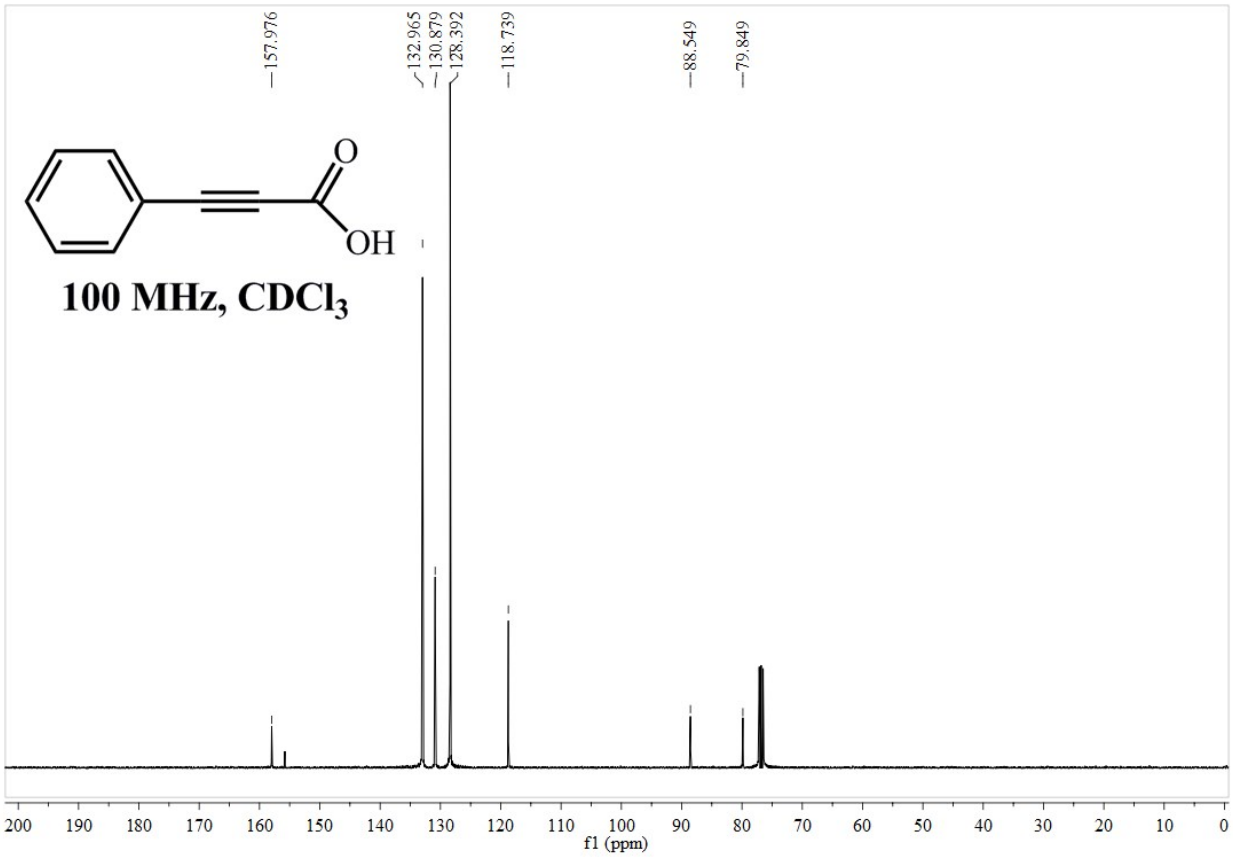
157.976
132.965
130.879
128.392
118.739
88.549
79.849
O
OH
100 MHz, CDCl3
200 190 180 170 160 150 140 130 120 110 100 90 80 70 60 50 40 30 20 10 0
f1 (ppm)

Compound **2**

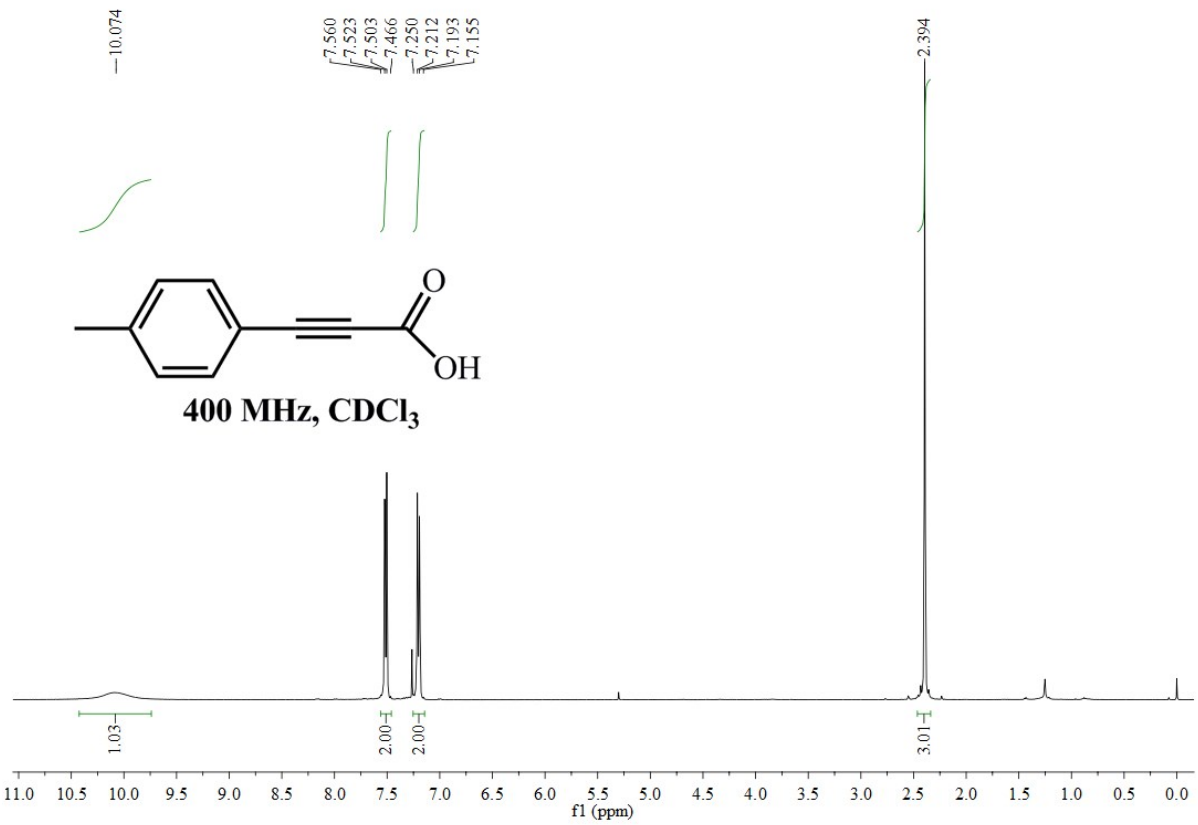
10.074
7.560
7.523
7.503
7.466
7.250
7.212
7.193
7.155
2.394
O
OH
400 MHz, CDCl3
1.03
2.00
2.00
3.01
11.0 10.5 10.0 9.5 9.0 8.5 8.0 7.5 7.0 6.5 6.0 5.5 5.0 4.5 4.0 3.5 3.0 2.5 2.0 1.5 1.0 0.5 0.0
f1 (ppm)

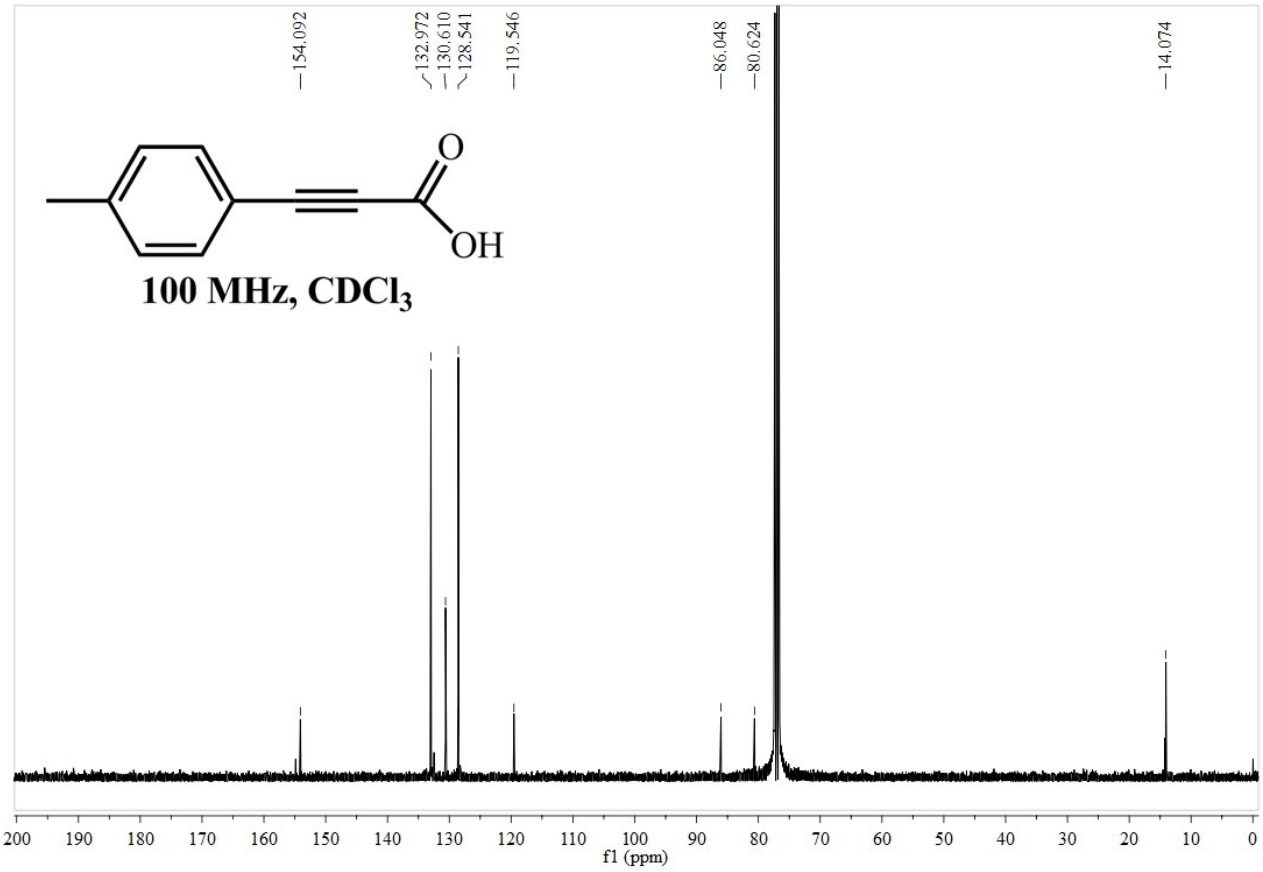
154.092
132.972
130.610
128.541
119.546
86.048
80.624
14.074
O
OH
100 MHz, CDCl3
f1 (ppm)

Compound **3**

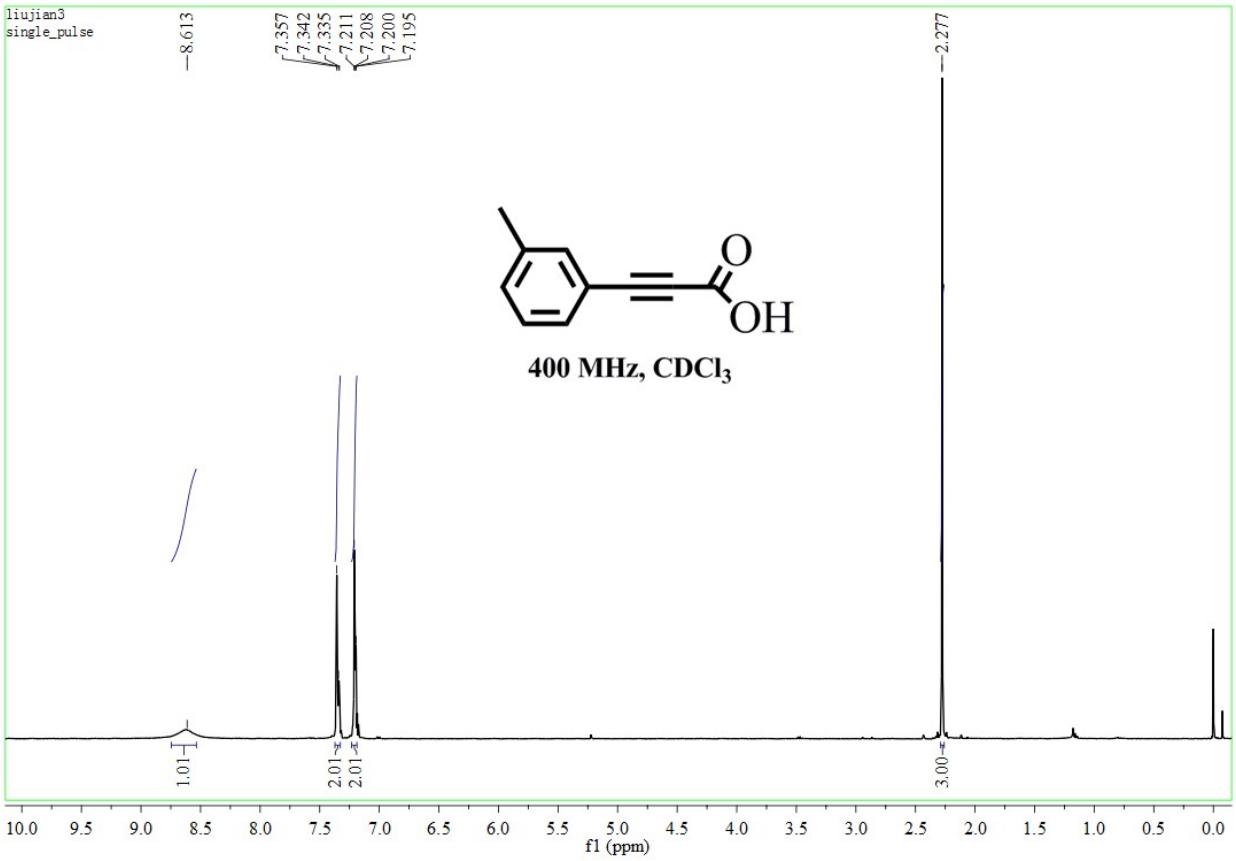
liujian3
single_pulse
8.613
7.357
7.342
7.335
7.211
7.208
7.200
7.195
2.277
O
OH
400 MHz, CDCl3
1.01
2.01
2.01
3.00
f1 (ppm)

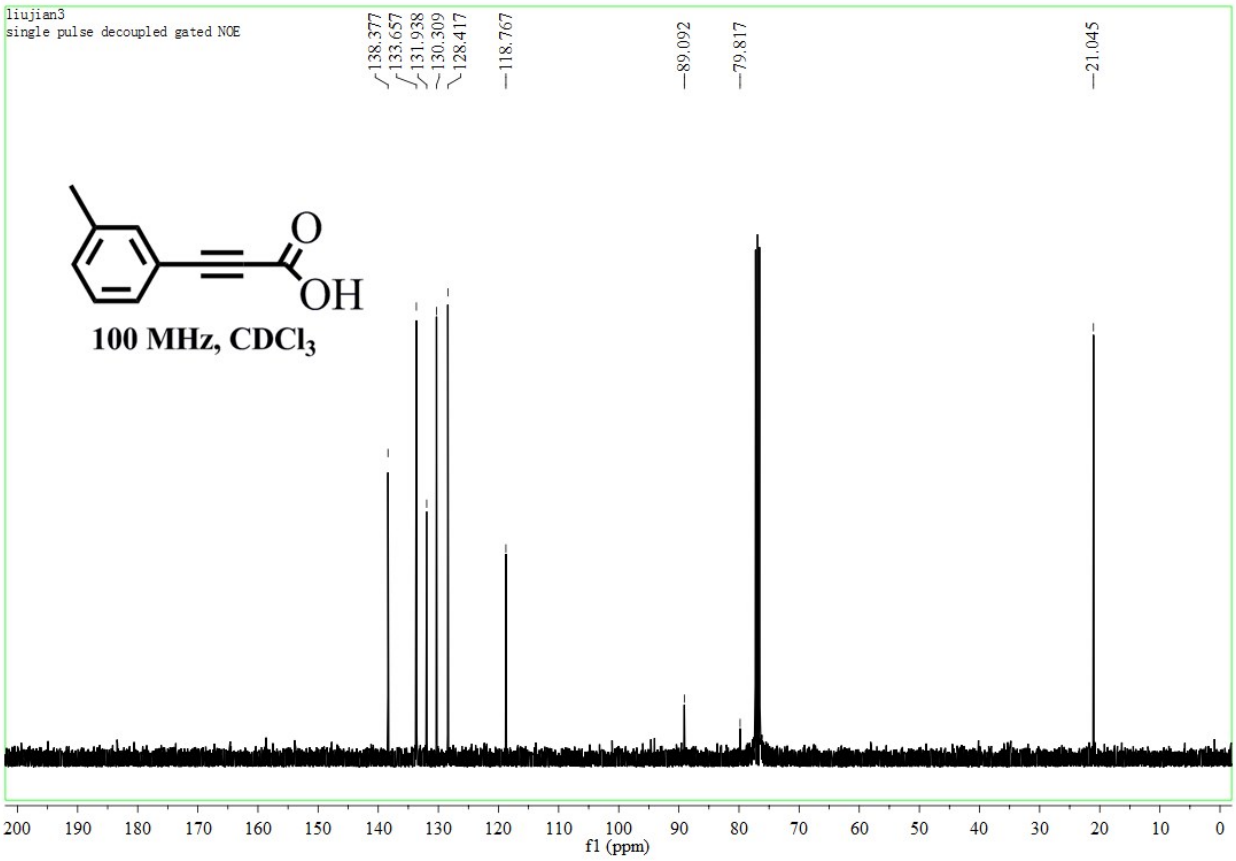
liujian3
single pulse decoupled gated NOE
138.377
133.657
131.938
130.309
128.417
118.767
89.092
79.817
21.045
O
OH
100 MHz, CDCl3
200 190 180 170 160 150 140 130 120 110 100 90 80 70 60 50 40 30 20 10 0
f1 (ppm)

Compound **4**

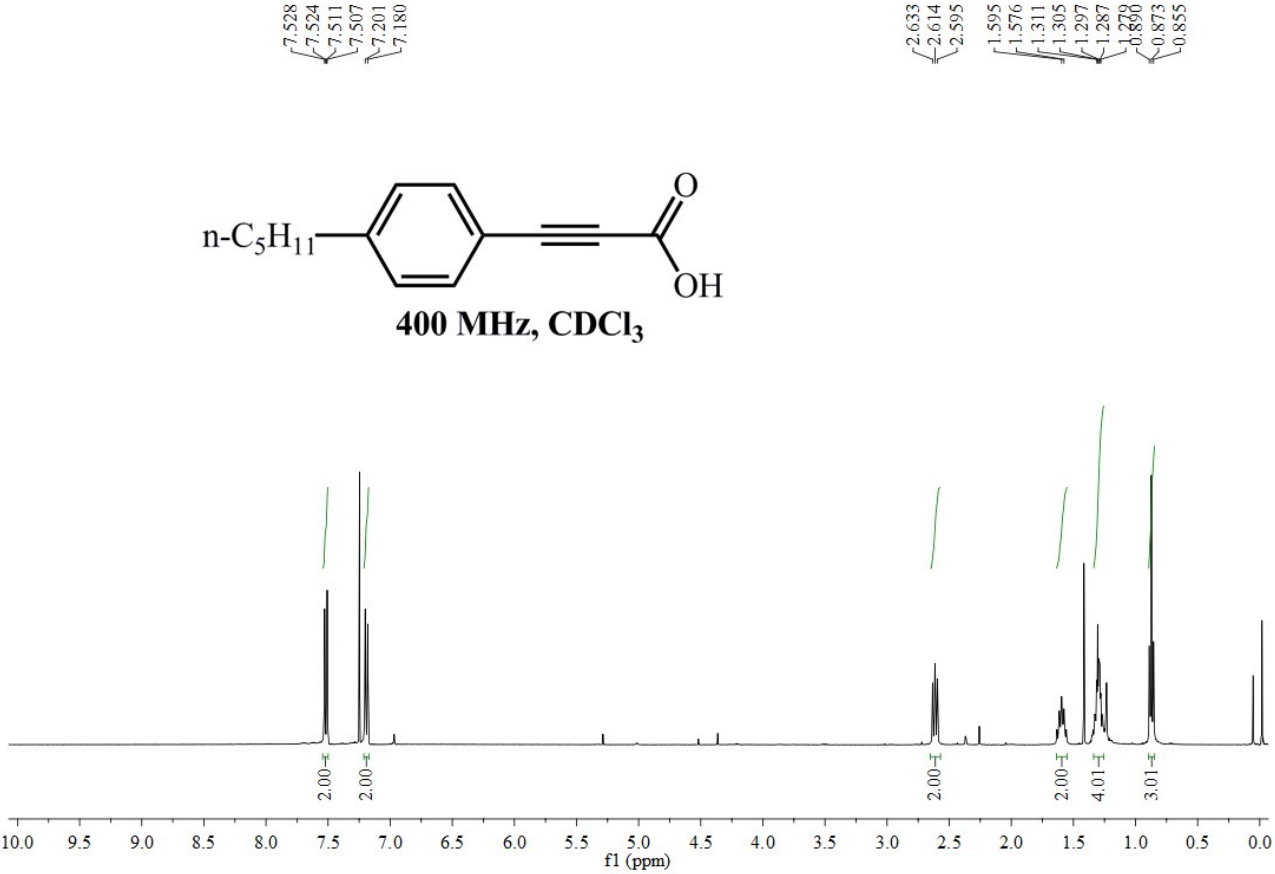
7.528
7.524
7.511
7.507
7.201
7.180
2.633
2.614
2.595
1.595
1.576
1.311
1.305
1.297
1.287
0.873
0.855
n-C5H11
O
OH
400 MHz, CDCl3
2.00
2.00
2.00
2.00
4.01
3.01
10.0 9.5 9.0 8.5 8.0 7.5 7.0 6.5 6.0 5.5 5.0 4.5 4.0 3.5 3.0 2.5 2.0 1.5 1.0 0.5 0.0
f1 (ppm)

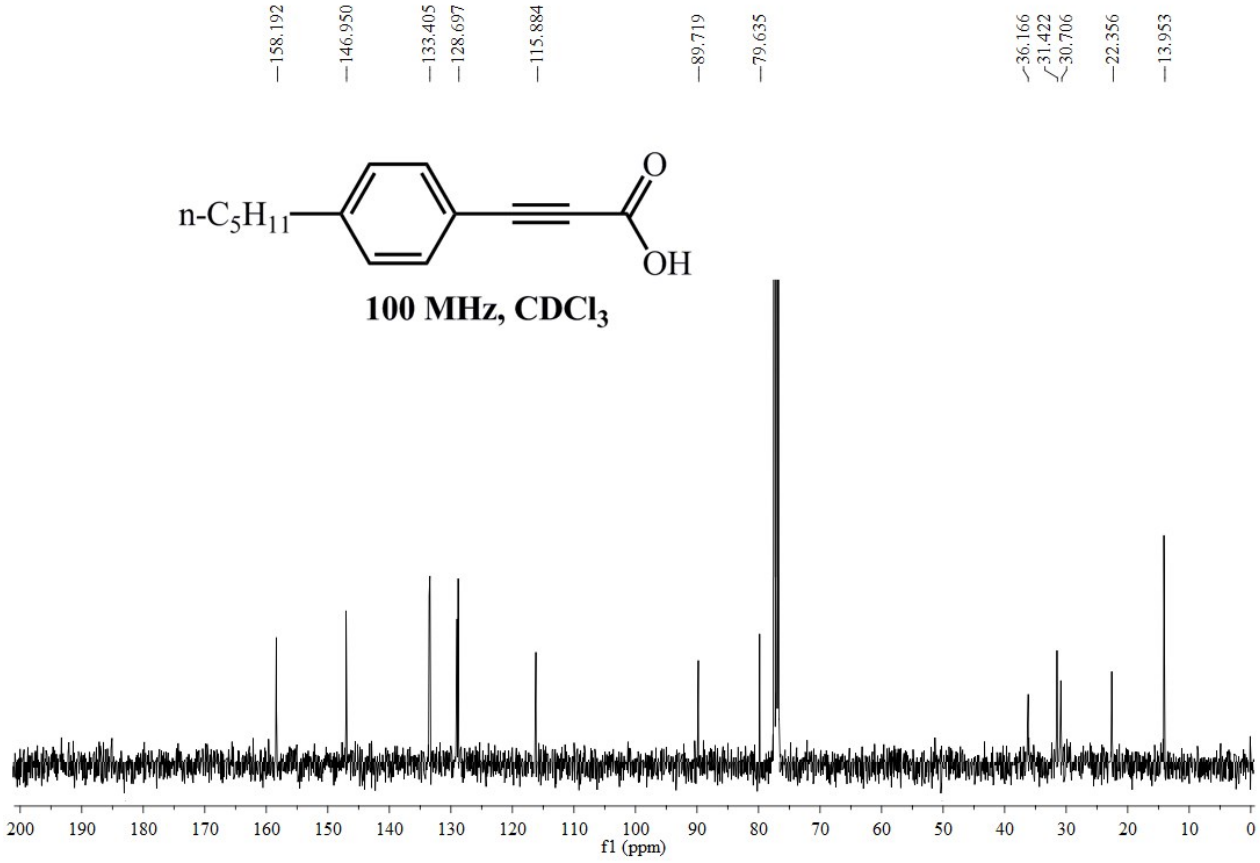
158.192
146.950
133.405
128.697
115.884
89.719
79.635
36.166
31.422
30.706
22.356
13.953
n-C5H11
O
OH
100 MHz, CDCl3
200 190 180 170 160 150 140 130 120 110 100 90 80 70 60 50 40 30 20 10 0
f1 (ppm)

Compound **5**

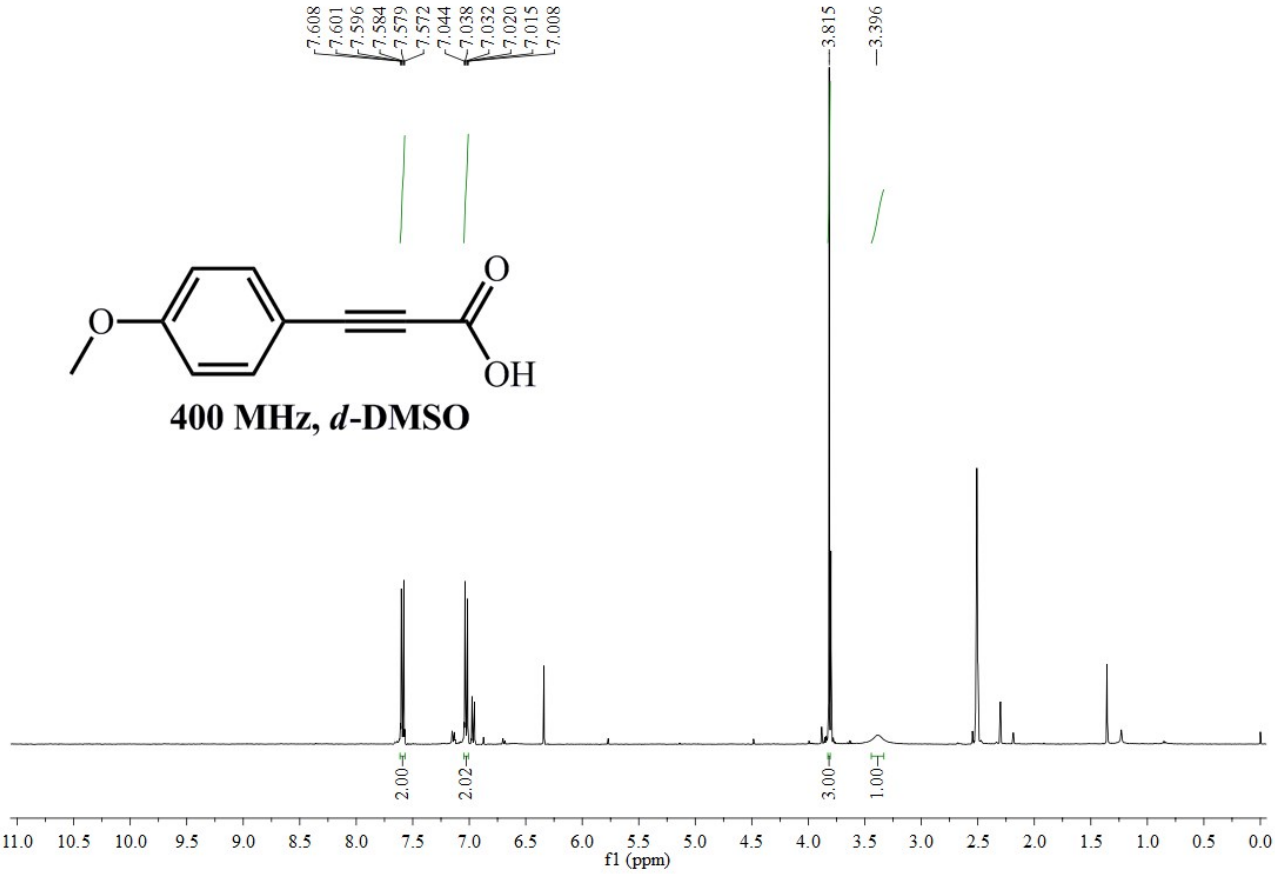
7.608
7.601
7.596
7.584
7.579
7.572
7.044
7.038
7.032
7.020
7.015
7.008
3.815
3.396
O
O
OH
400 MHz, *d*-DMSO
2.00
2.02
3.00
1.00
11.0 10.5 10.0 9.5 9.0 8.5 8.0 7.5 7.0 6.5 6.0 5.5 5.0 4.5 4.0 3.5 3.0 2.5 2.0 1.5 1.0 0.5 0.0
f1 (ppm)

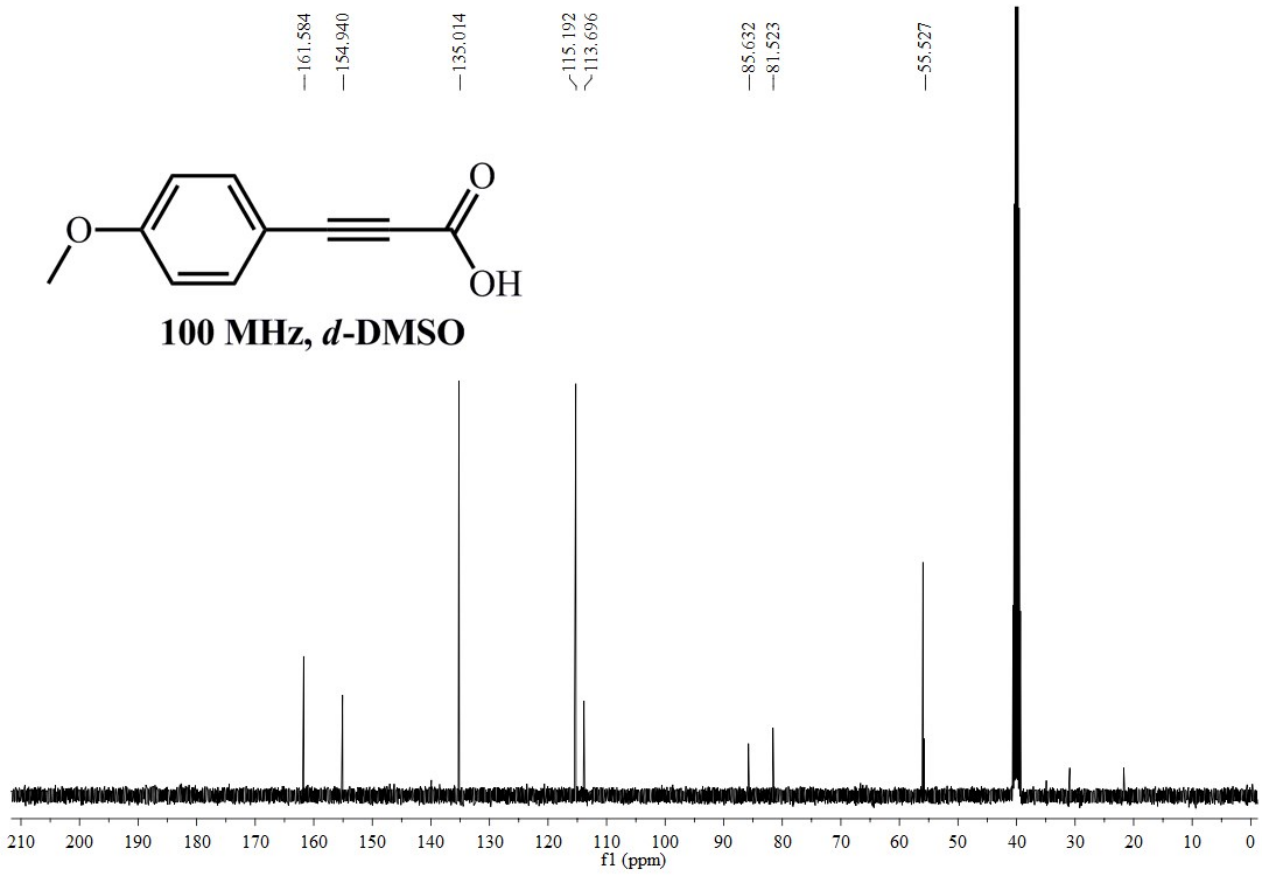
161.584
154.940
135.014
115.192
113.696
85.632
81.523
55.527
O
O
OH
100 MHz, *d*-DMSO
210 200 190 180 170 160 150 140 130 120 110 100 90 80 70 60 50 40 30 20 10 0
f1 (ppm)

Compound **6**

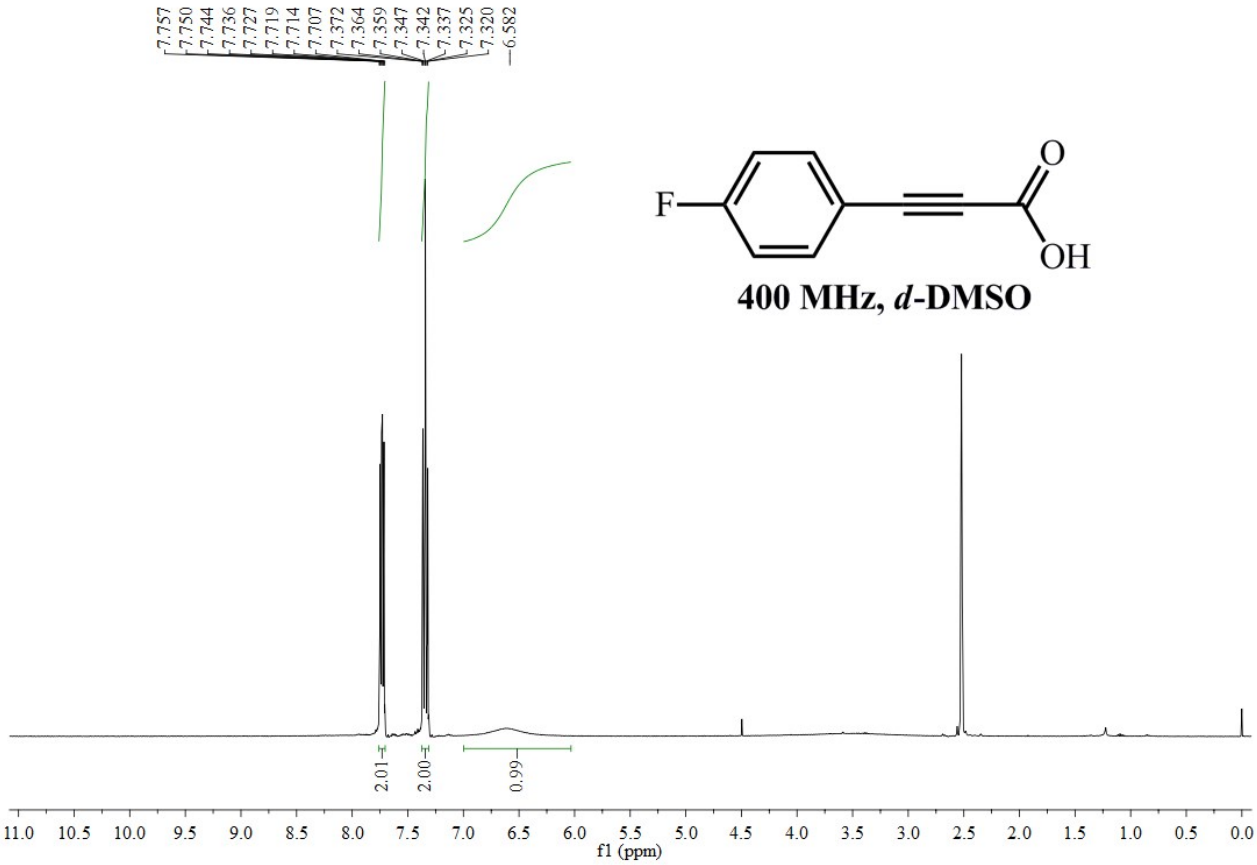
7.757
7.750
7.744
7.736
7.727
7.719
7.714
7.707
7.372
7.364
7.359
7.347
7.342
7.337
7.325
7.320
6.582
F
O
OH
400 MHz, d-DMSO
2.01
2.00
0.99
11.0 10.5 10.0 9.5 9.0 8.5 8.0 7.5 7.0 6.5 6.0 5.5 5.0 4.5 4.0 3.5 3.0 2.5 2.0 1.5 1.0 0.5 0.0
f1 (ppm)

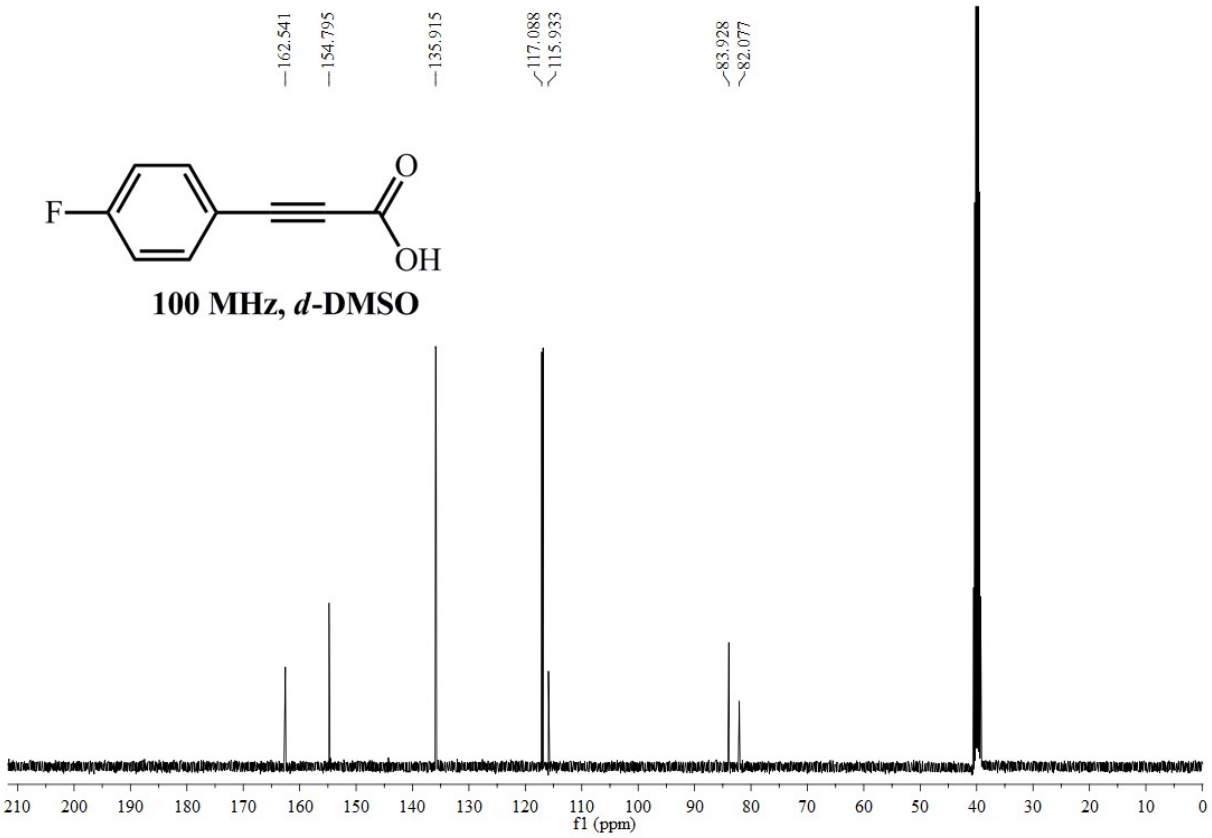
162.541
154.795
135.915
117.088
115.933
83.928
82.077
F
O
OH
100 MHz, d-DMSO
210 200 190 180 170 160 150 140 130 120 110 100 90 80 70 60 50 40 30 20 10 0
f1 (ppm)

Compound **7**

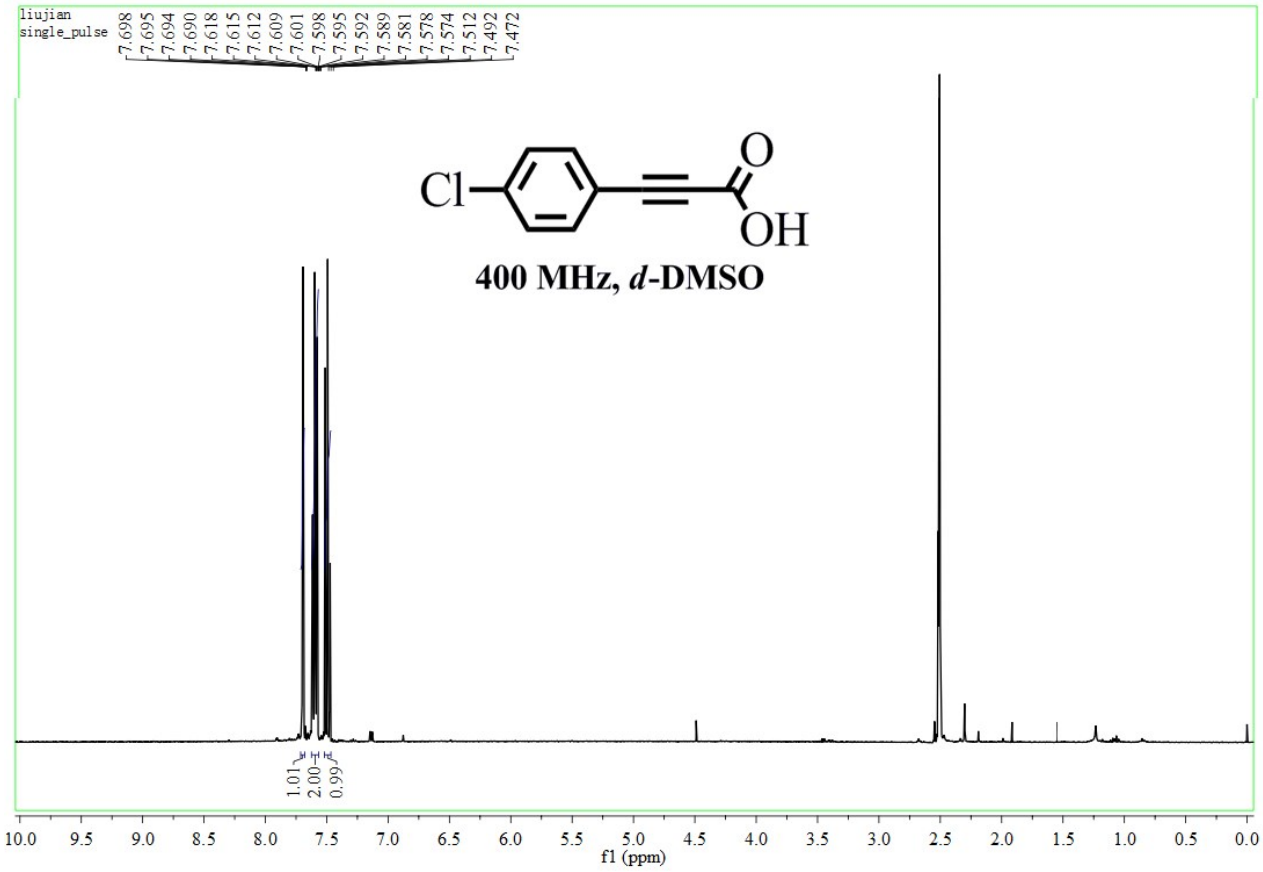
liujian
single_pulse
7.698
7.695
7.694
7.690
7.618
7.615
7.612
7.609
7.601
7.598
7.595
7.592
7.589
7.581
7.578
7.574
7.512
7.492
7.472
Cl
O
OH
400 MHz, d-DMSO
1.01
2.00
0.99
10.0 9.5 9.0 8.5 8.0 7.5 7.0 6.5 6.0 5.5 5.0 4.5 4.0 3.5 3.0 2.5 2.0 1.5 1.0 0.5 0.0
f1 (ppm)

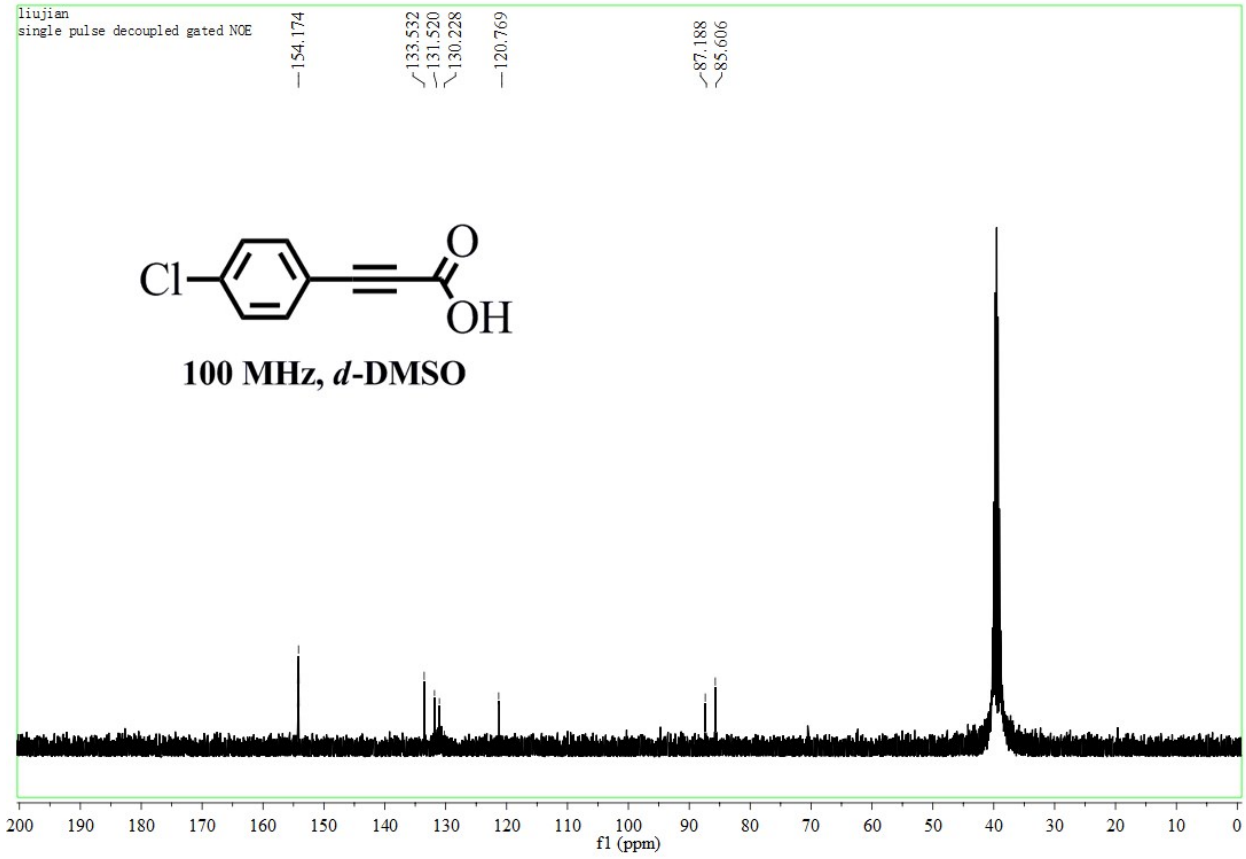
liujian
single pulse decoupled gated NOE
154.174
133.532
131.520
130.228
120.769
87.188
85.606
Cl
O
OH
100 MHz, d-DMSO
200 190 180 170 160 150 140 130 120 110 100 90 80 70 60 50 40 30 20 10 0
f1 (ppm)

Compound **8**

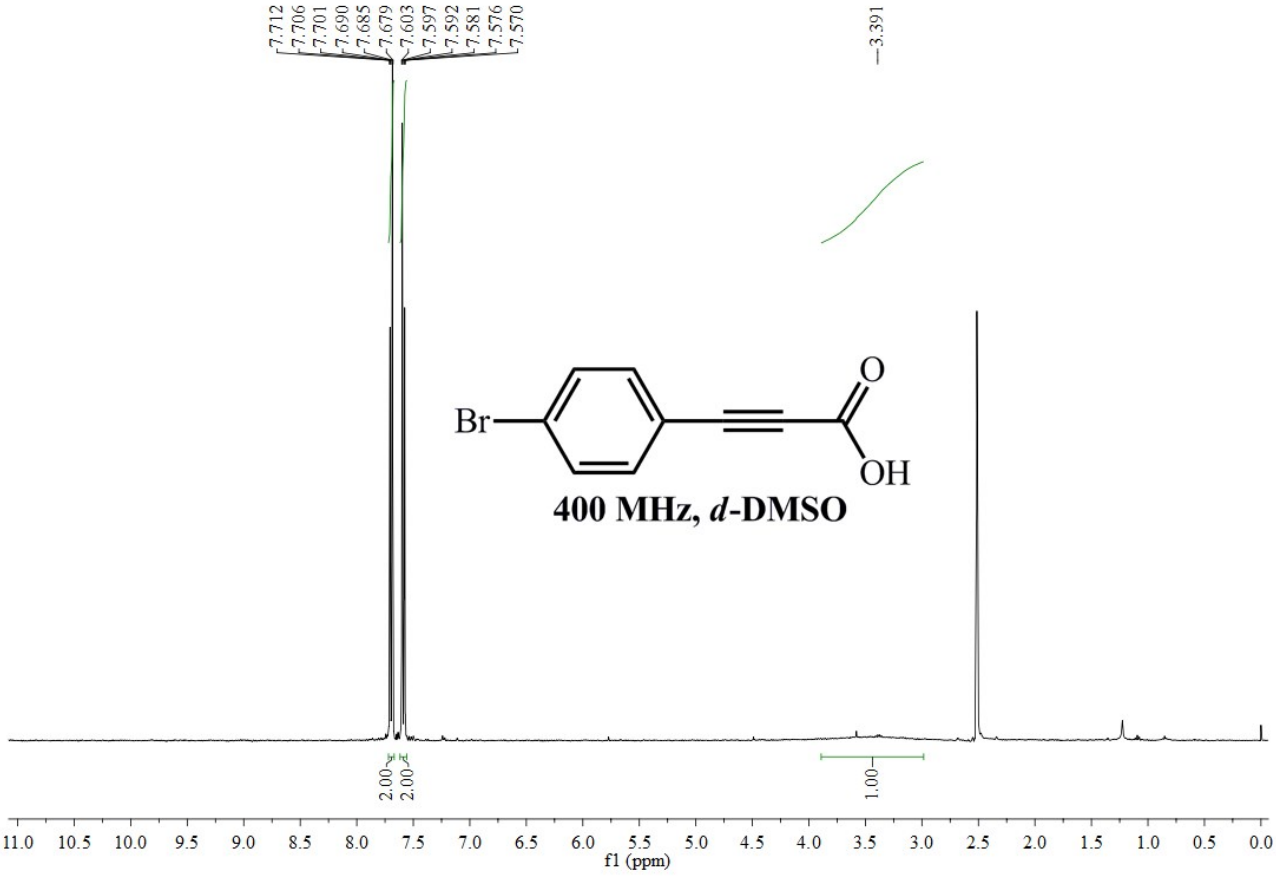
7.712
7.706
7.701
7.690
7.685
7.679
7.603
7.597
7.592
7.581
7.576
7.570
3.391
Br
O
OH
400 MHz, d-DMSO
2.00
2.00
1.00
11.0 10.5 10.0 9.5 9.0 8.5 8.0 7.5 7.0 6.5 6.0 5.5 5.0 4.5 4.0 3.5 3.0 2.5 2.0 1.5 1.0 0.5 0.0
f1 (ppm)

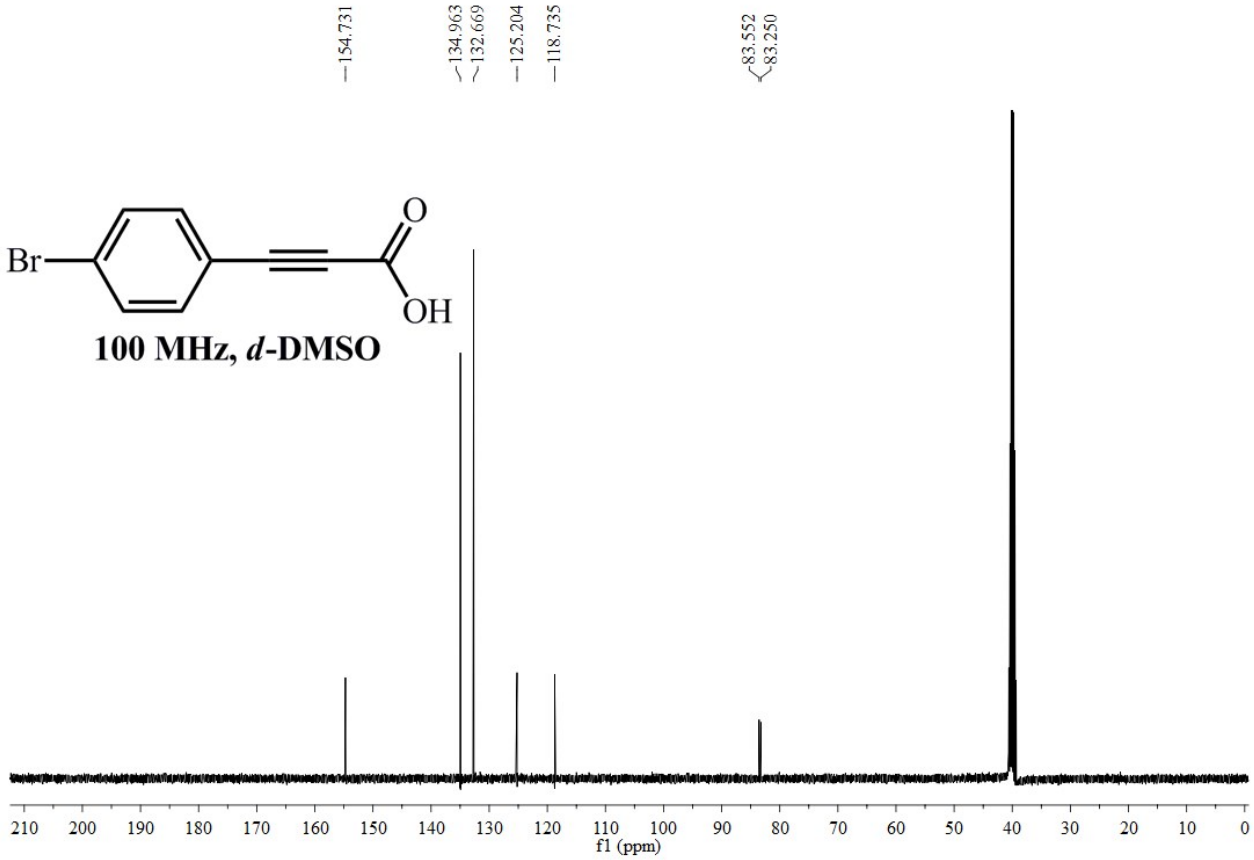
154.731
134.963
132.669
125.204
118.735
83.552
83.250
Br
O
OH
100 MHz, d-DMSO
210 200 190 180 170 160 150 140 130 120 110 100 90 80 70 60 50 40 30 20 10 0
f1 (ppm)

Compound **9**

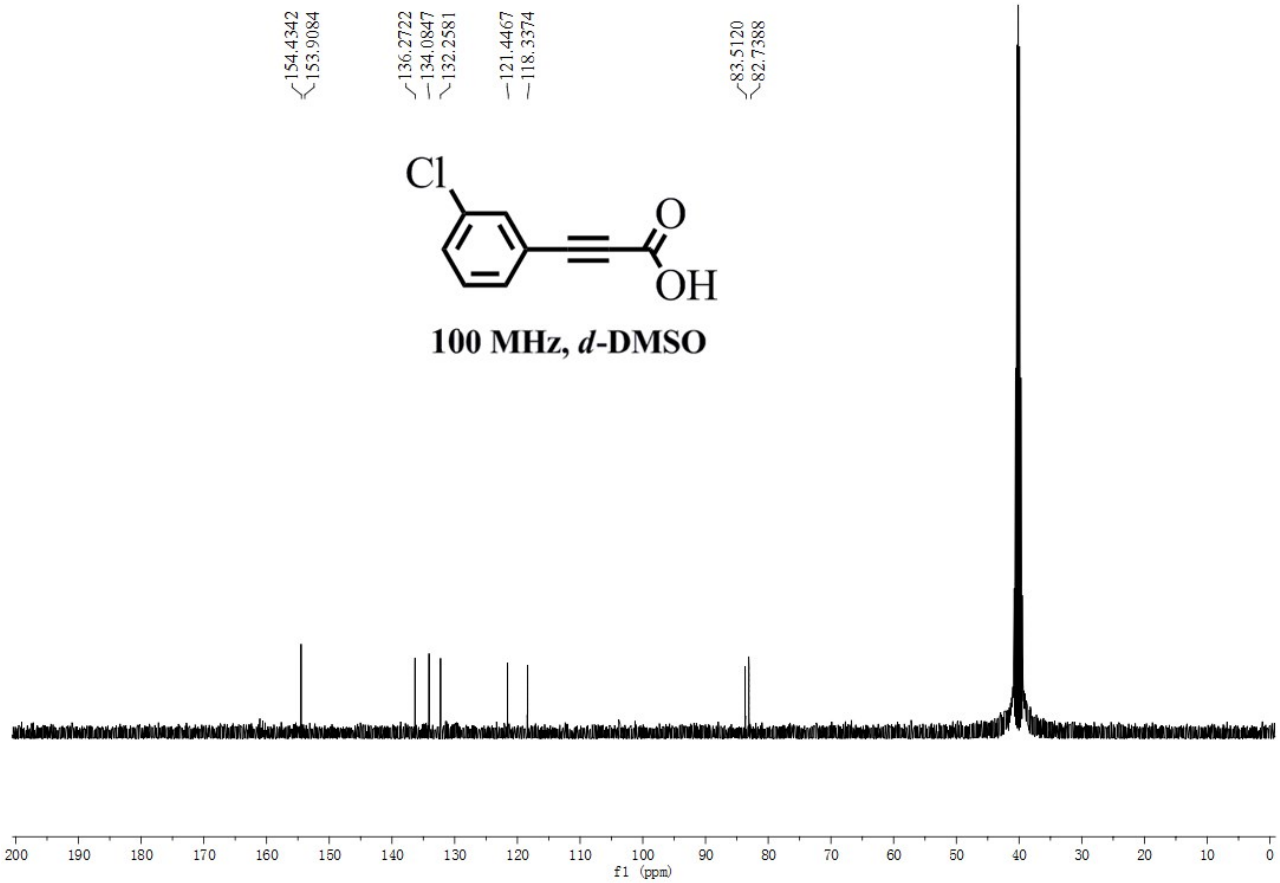
154.4342
153.9084
136.2722
134.0847
132.2581
121.4467
118.3374
83.5120
82.7388
Cl
O
OH
100 MHz, d-DMSO
f1 (ppm)

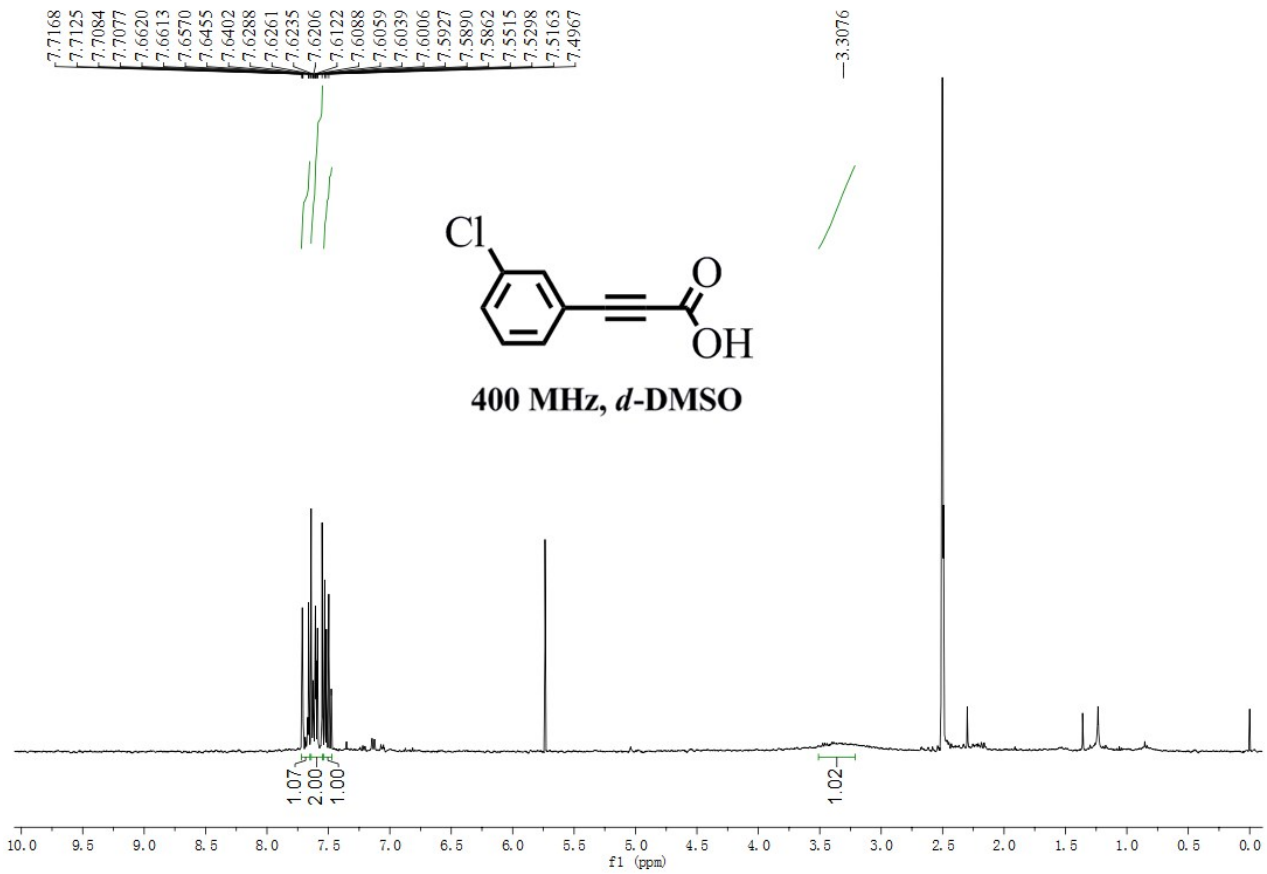
7.7168
7.7125
7.7084
7.7077
7.6620
7.6613
7.6570
7.6455
7.6402
7.6288
7.6261
7.6235
7.6206
7.6122
7.6088
7.6059
7.6039
7.6006
7.5927
7.5890
7.5862
7.5515
7.5298
7.5163
7.4967
3.3076
Cl
O
OH
400 MHz, d-DMSO
1.07
2.00
1.00
1.02
f1 (ppm)

Compound **10**

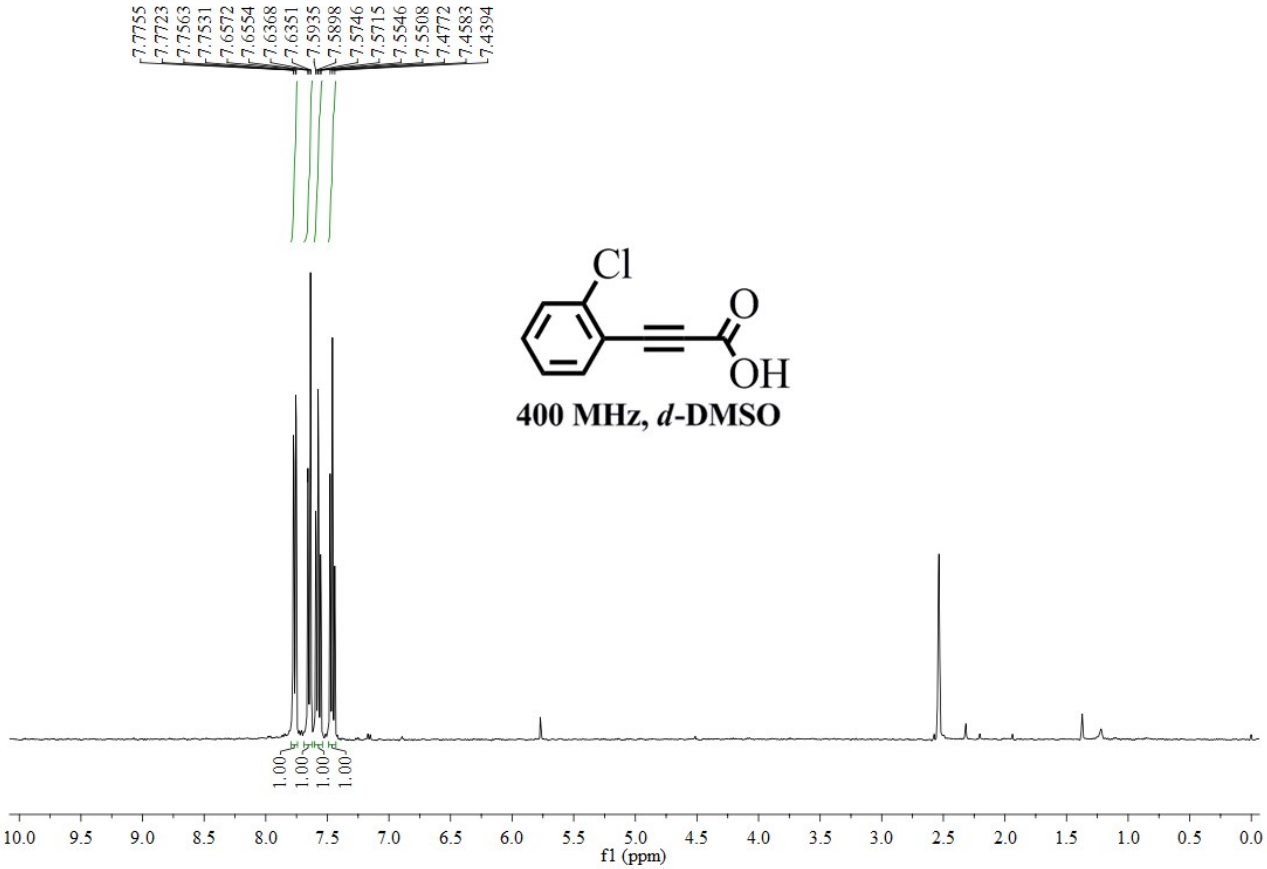
7.7755
7.7723
7.7563
7.7531
7.6572
7.6554
7.6368
7.6351
7.5935
7.5898
7.5746
7.5715
7.5546
7.5508
7.4772
7.4583
7.4394
Cl
O
OH
400 MHz, d-DMSO
1.00
1.00
1.00
1.00
10.0 9.5 9.0 8.5 8.0 7.5 7.0 6.5 6.0 5.5 5.0 4.5 4.0 3.5 3.0 2.5 2.0 1.5 1.0 0.5 0.0
f1 (ppm)

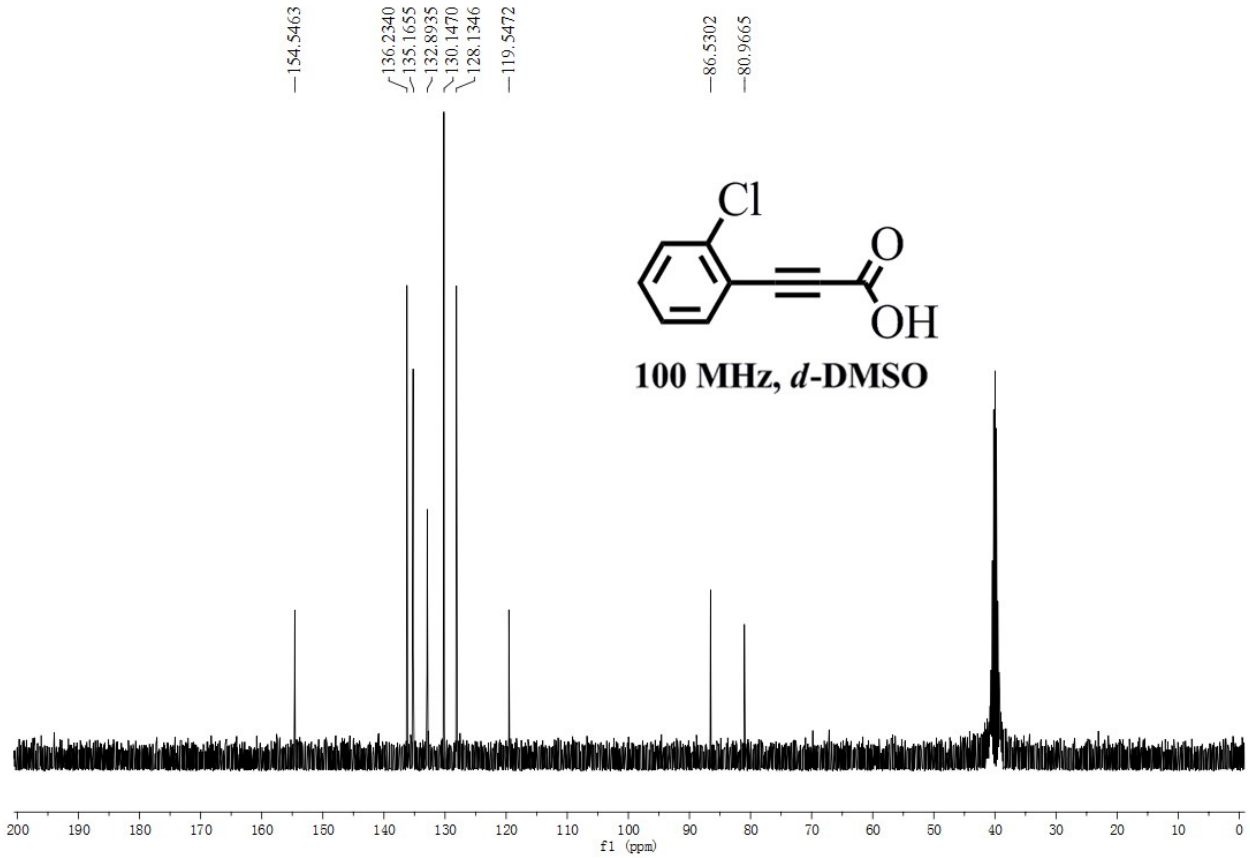
154.5463
136.2340
135.1655
132.8935
130.1470
128.1346
119.5472
86.5302
80.9665
Cl
O
OH
100 MHz, d-DMSO
200 190 180 170 160 150 140 130 120 110 100 90 80 70 60 50 40 30 20 10 0
f1 (ppm)

Compound **11**

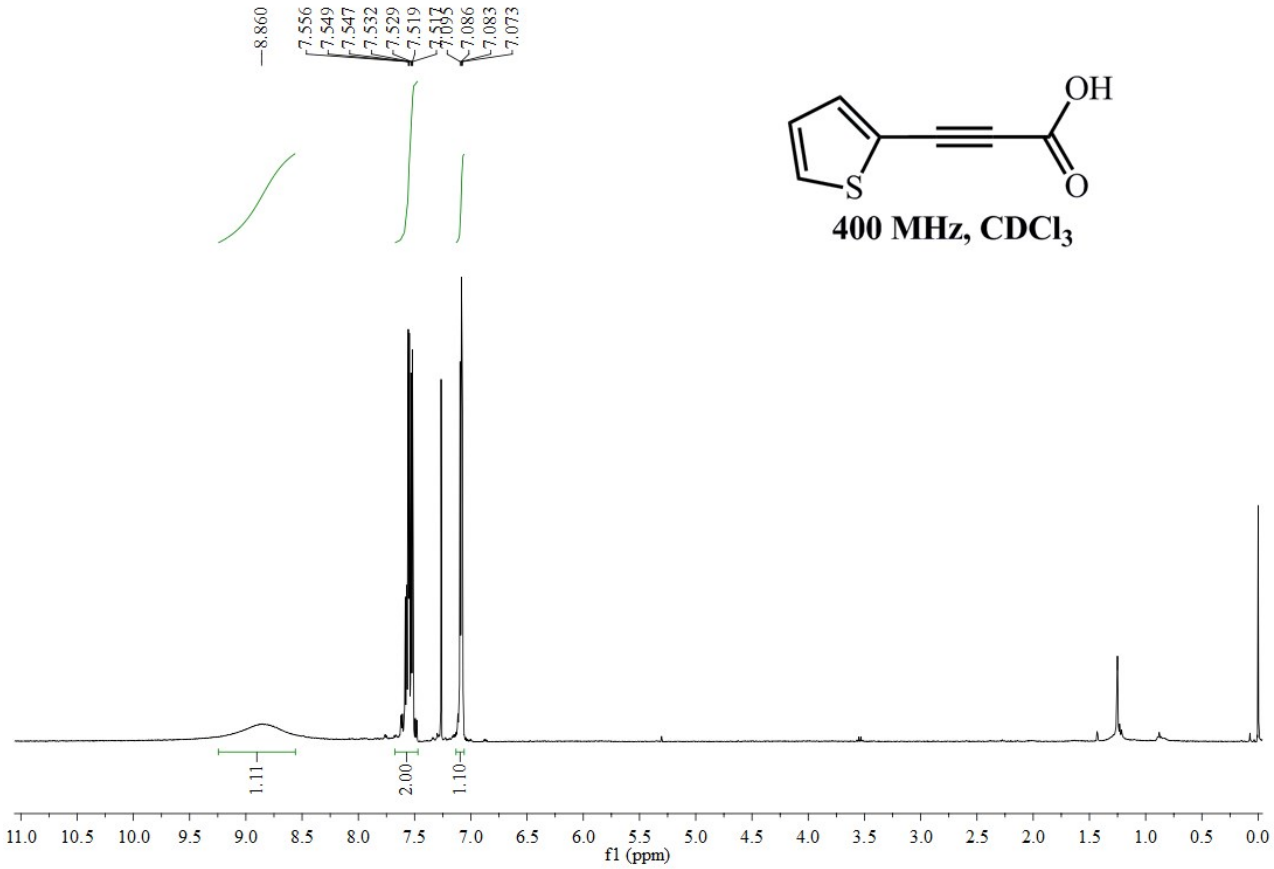
8.860
7.556
7.549
7.547
7.532
7.529
7.519
7.086
7.083
7.073
OH
S
O
400 MHz, CDCl3
1.11
2.00
1.10
f1 (ppm)

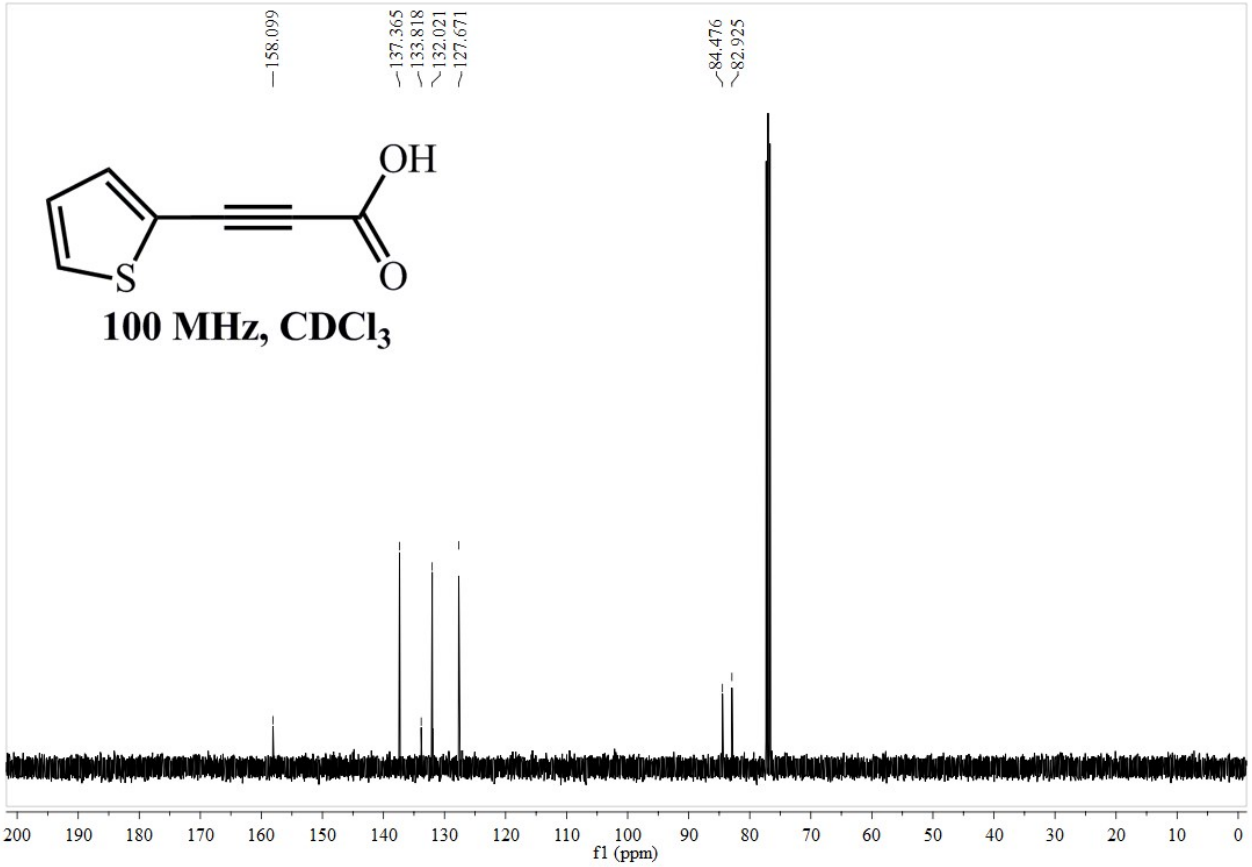
158.099
137.365
133.818
132.021
127.671
84.476
82.925
OH
S
O
100 MHz, CDCl3
f1 (ppm)

Compound **12**

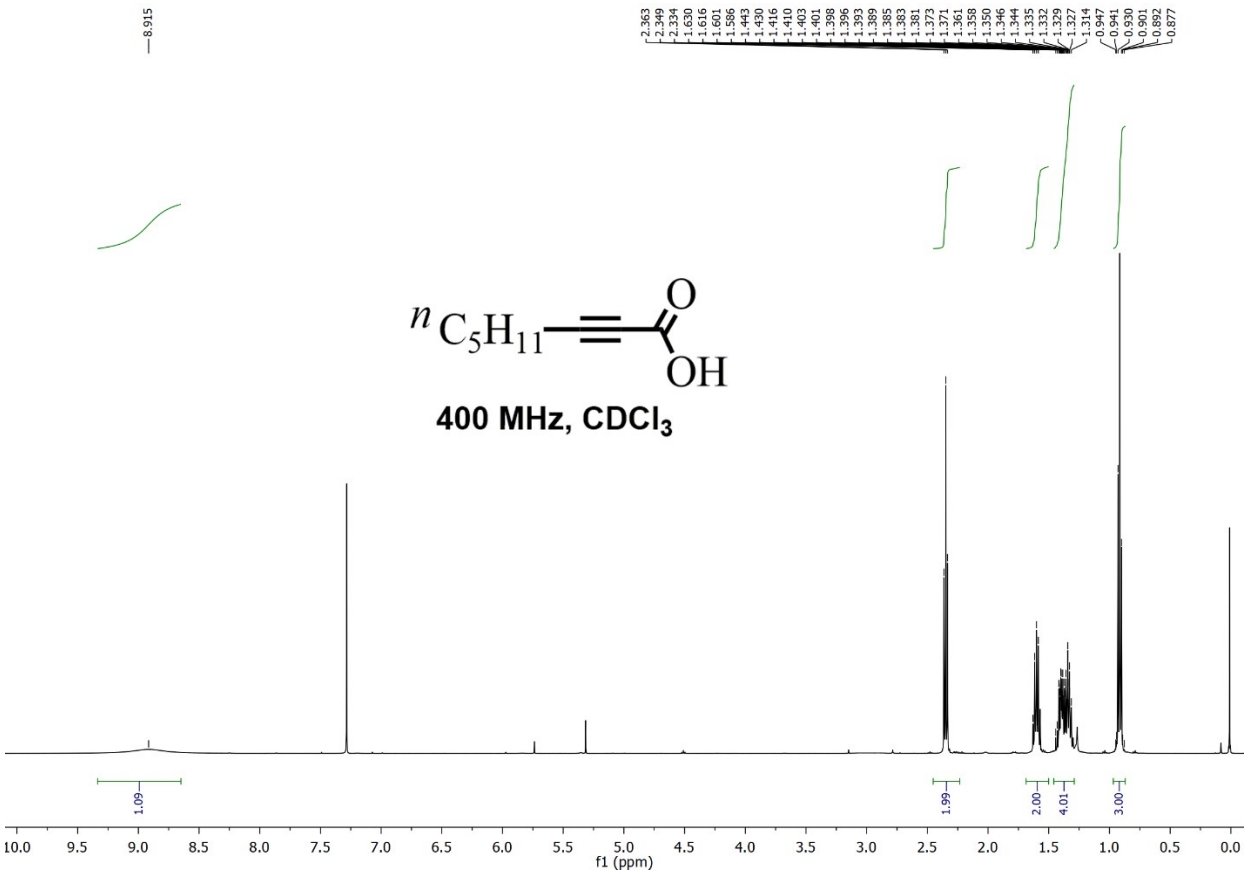
8.915
2.363
2.349
2.334
2.630
1.616
1.601
1.586
1.443
1.430
1.420
1.416
1.410
1.403
1.401
1.398
1.396
1.393
1.389
1.385
1.383
1.381
1.373
1.371
1.361
1.358
1.350
1.346
1.344
1.335
1.332
1.329
1.327
1.314
0.947
0.941
0.930
0.901
0.892
0.877
$^{n}C_5H_{11}$
O
OH
400 MHz, $CDCl_3$
1.09
1.99
2.00
4.01
3.00
10.0 9.5 9.0 8.5 8.0 7.5 7.0 6.5 6.0 5.5 5.0 4.5 4.0 3.5 3.0 2.5 2.0 1.5 1.0 0.5 0.0
f1 (ppm)

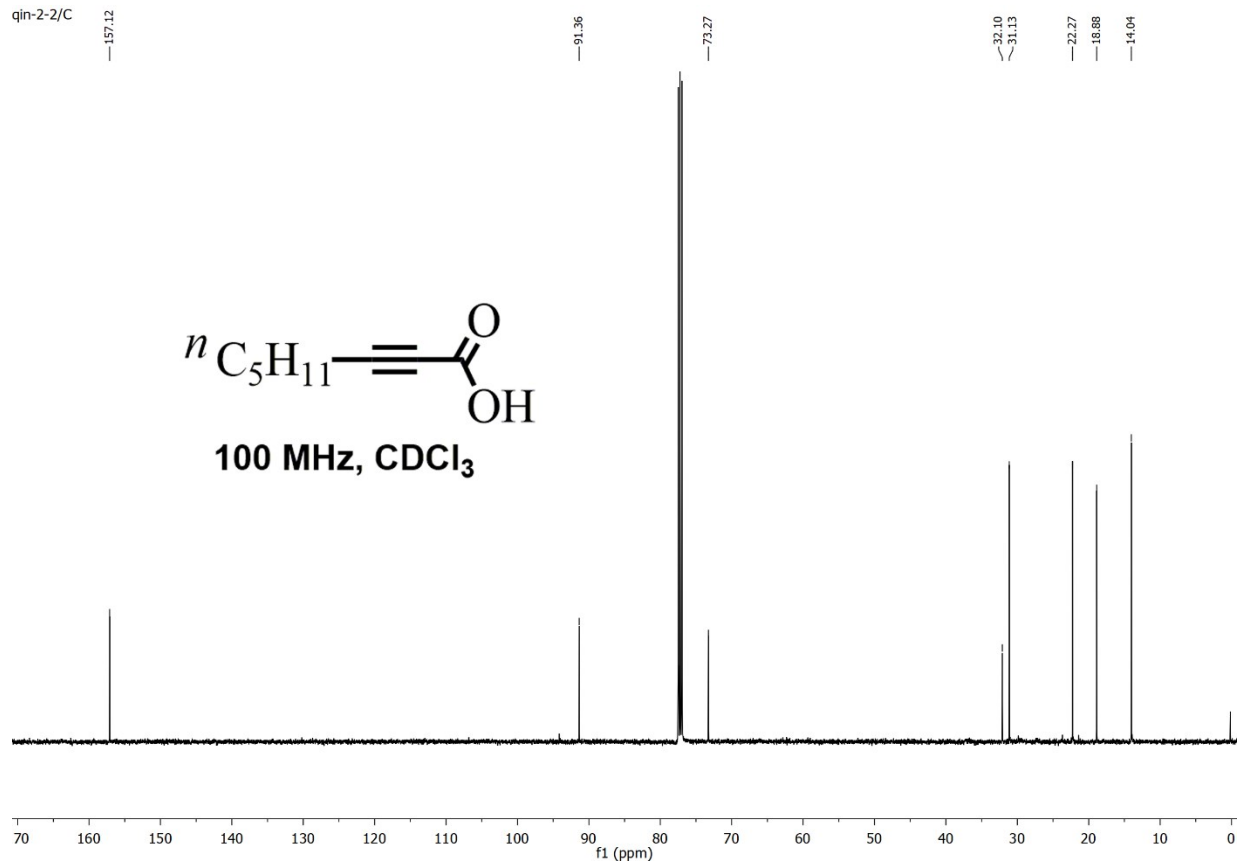
qin-2-2/C
157.12
91.36
73.27
32.10
31.13
22.27
18.88
14.04
$^{n}C_5H_{11}$
O
OH
100 MHz, $CDCl_3$
70 160 150 140 130 120 110 100 90 80 70 60 50 40 30 20 10 0
f1 (ppm)

Compound **13**

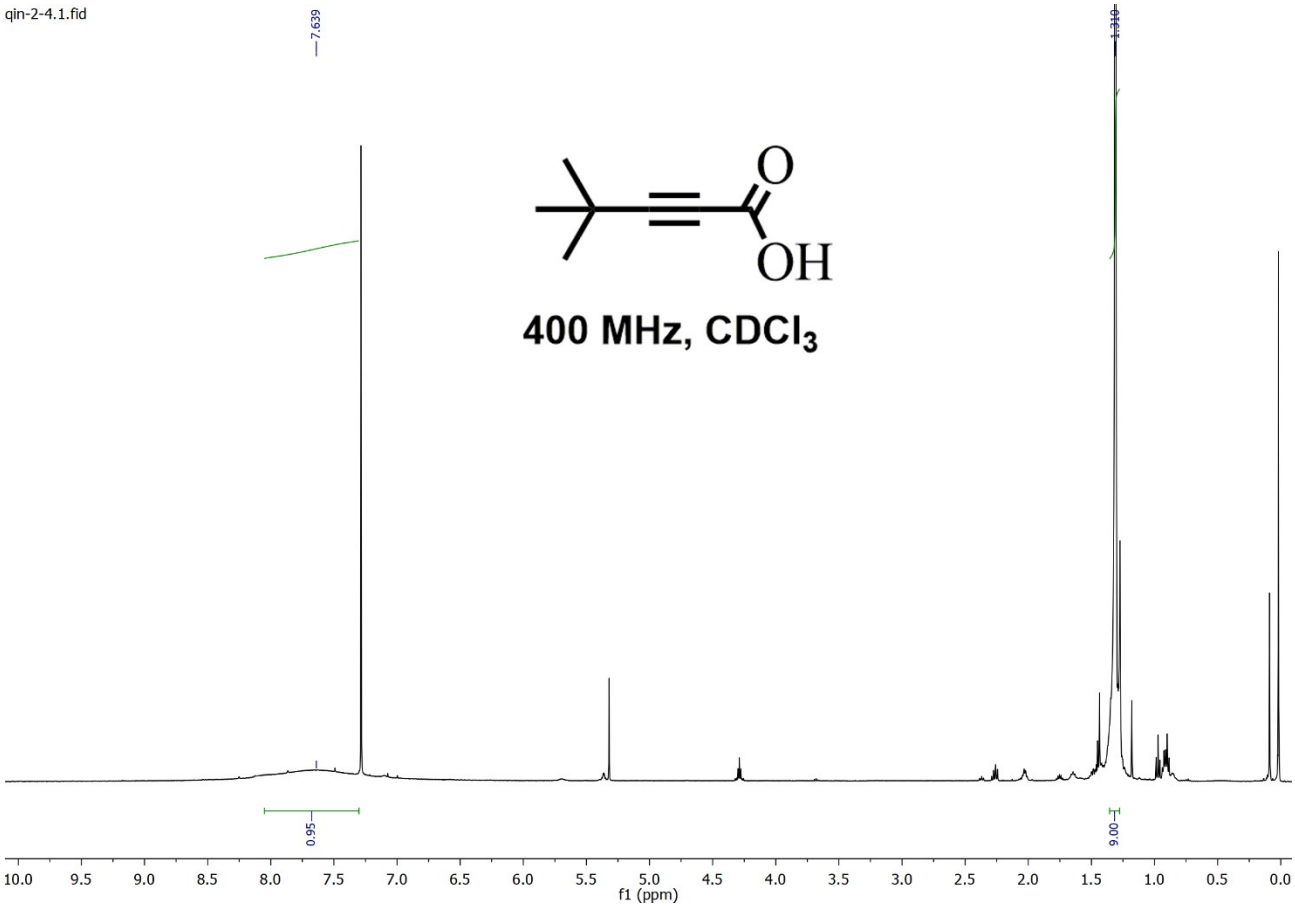
qin-2-4.1.fid
7.639
1.319
O
OH
400 MHz, CDCl3
0.95
9.00
10.0 9.5 9.0 8.5 8.0 7.5 7.0 6.5 6.0 5.5 5.0 4.5 4.0 3.5 3.0 2.5 2.0 1.5 1.0 0.5 0.0
f1 (ppm)

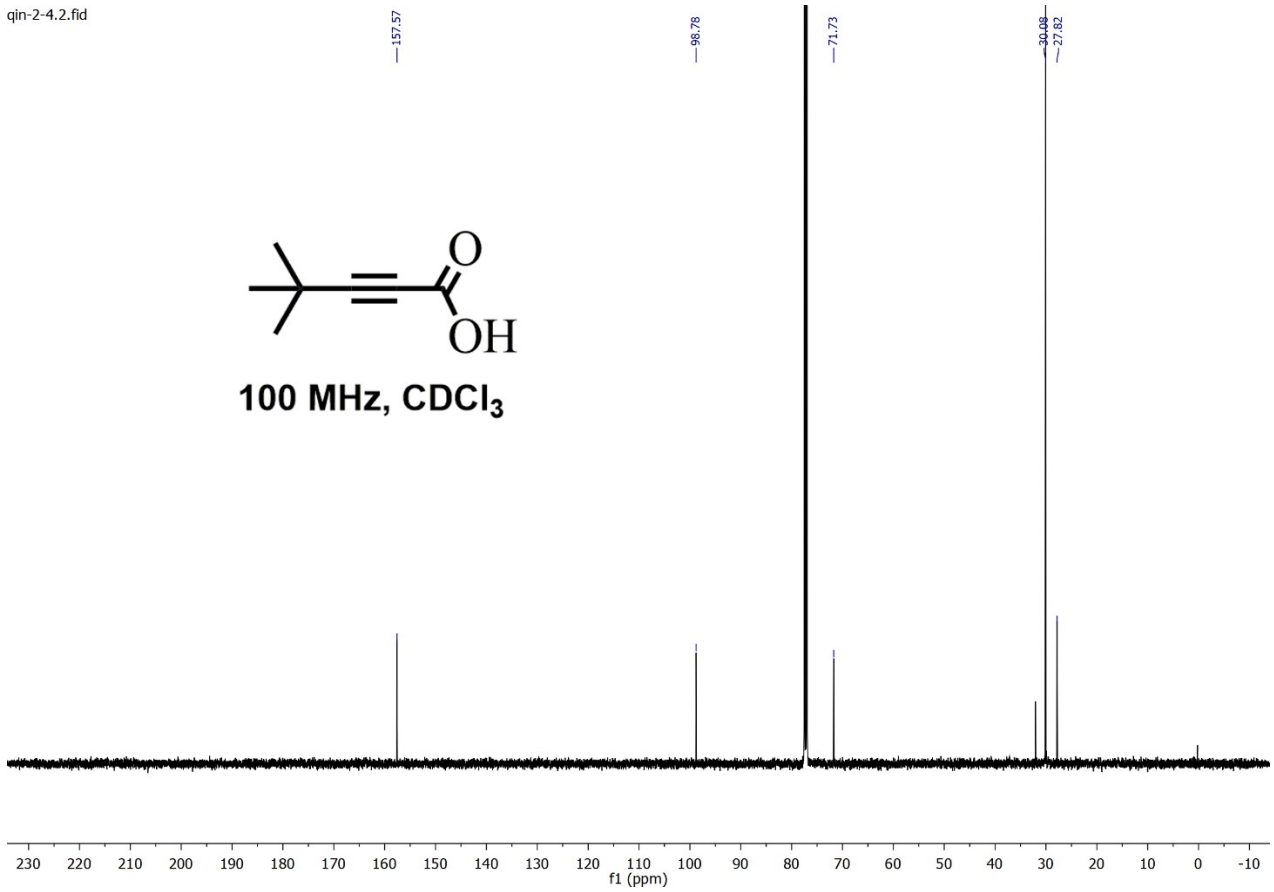
qin-2-4.2.fid
157.57
98.78
71.73
30.08
27.82
O
OH
100 MHz, CDCl3
230 220 210 200 190 180 170 160 150 140 130 120 110 100 90 80 70 60 50 40 30 20 10 0 -10
f1 (ppm)